Ingeniería y Competitividad
Vol 28 (3) 2026 doi: 10.25100/iyc.v28i3.16035

Vol 28 (3)

ISSN
0123-3033
e- 2027-8284

Original Article

Quantification of instantaneous complex power p-q considering balanced three-phase loads

Cuantificación de la potencia compleja instantánea p-q considerando cargas trifásicas equilibradas

Julián García-Guarin[1] Edison Andrés Caicedo-Peñaranda[1]

[1]Grupo de Investigación en Sistemas Energéticos, Programa de Ingeniería Eléctrica, Universidad de Pamplona. Norte de Santander, Colombia.

Abstract

Introduction: the p-q power theory covers balanced three-phase systems and is fundamental to analyzing energy flow in smart electrical grids. The traditional approach, based on root mean square (RMS) values, allows average power to be calculated, whereas the time-domain formulation enables the analysis of instantaneous power and its periodic variation between positive and negative cycles. However, this approach does not distinguish between energy converted into useful work and energy that simply oscillates between the source and the load.
Objective: to quantify instantaneous active and reactive power by comparing four estimation methods.
Methodology: four methods were compared: p-q theory based on the Clarke transform, the Hilbert transform, estimation using the dot product (p) and cross product (q), and the two-wattmeter method. Four types of loads were evaluated: resistive, resistive-inductive, capacitive-resistive, and nonlinear. The estimates were compared with reference values obtained using Simscape/MATLAB, employing maximum error, mean squared error, mean absolute error, and absolute and relative errors of instantaneous complex power as evaluation metrics.
Results: the methods exhibited similar behavioral patterns and converged toward the average values of complex power. For linear loads, relative errors were below 0.62% for active power and 0.33% for reactive power. Additionally, low-pass filtering helped reduce unwanted oscillations.
Conclusions: the evaluated methods exhibit similar performance in estimating instantaneous active and reactive power, with relative errors below 1% for linear loads.

Keywords: Aron circuit, active and reactive power estimation, instantaneous complex power filters, three-phase power measurement.

Resumen

Introducción: la teoría de potencia p-q abarca los sistemas trifásicos equilibrados y resulta fundamental para analizar el flujo de energía en las redes eléctricas inteligentes. El enfoque tradicional, basado en valores eficaces (RMS), permite calcular la potencia media, mientras que la formulación en el dominio del tiempo permite analizar la potencia instantánea y su variación periódica entre ciclos positivos y negativos. Sin embargo, este enfoque no distingue la energía transformada en trabajo útil de aquella que oscila entre la fuente y la carga.
Objetivo: cuantificar la potencia activa y reactiva instantáneas mediante la comparación de cuatro métodos de estimación.
Metodología: se compararon cuatro métodos: teoría p-q basada en la transformada de Clarke, transformada de Hilbert, estimación mediante producto escalar (p) y producto vectorial (q), y método de los dos vatímetros. Se evaluaron cuatro tipos de cargas: resistivas, resistivo-inductivas, capacitivo-resistivas y no lineales. Las estimaciones se contrastaron con valores de referencia obtenidos mediante Simscape/MATLAB, utilizando indicadores de error máximo, error cuadrático medio, error absoluto medio y errores absolutos y relativos de las potencias instantáneas complejas.
Resultados: los métodos presentaron patrones de comportamiento similares y convergencia hacia los valores medios de la potencia compleja. En cargas lineales, los errores relativos fueron inferiores al 0,62 % para la potencia activa y al 0,33 % para la reactiva. Además, el filtrado paso bajo contribuyó a reducir las oscilaciones no deseadas.
Conclusiones: los métodos evaluados presentan comportamientos similares en la estimación de las potencias activa y reactiva instantáneas, con errores relativos inferiores al 1 % en cargas lineales.

Palabras clave: Circuito Aron, estimación de potencia activa y reactiva, filtros para potencia compleja instantánea, medición de potencia trifásica.

How to cite?

García.Guarin J, Caicedo-Peñaranda EA. Quantification of instantaneous complex power p-q considering balanced three-phase loads Ingeniería y Competitividad, 2026, 28(3)e-20716035

https://doi.org/10.25100/iyc.v28i3.16035

Received: 25/7/26
Reviewed: 15/9/26
Accepted: 23/11/26
Online: 26/11/26

Correspondence

pedro.garcia25@unipamplona.edu.co

Spanish version

CrossMark

CC BY NC SA

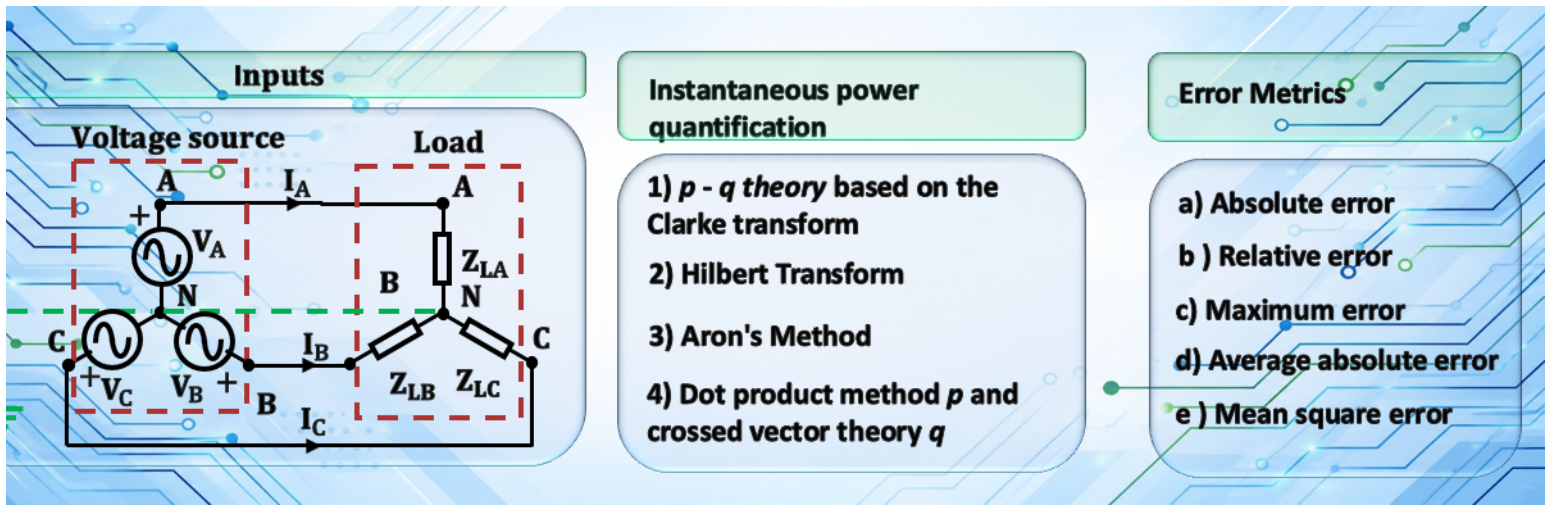
OPEN ACCESS

Why was the study conducted?
To quantify instantaneous active and reactive power in balanced three-phase systems by comparing four different methodologies: 1) Clarke-based theory, 2) the Hilbert transform, 3) the dot product and cross product theory, and 4) the two-wattmeter method

What were the key findings?
The evaluated methods converge toward average power values, showing relative errors below 0.62% for active power and 0.33% for reactive power under linear load conditions.
Nonlinear loads present the greatest challenge to measurement accuracy due to harmonic distortion.
The integration of second-order low-pass filters with a Butterworth response is crucial across all methodologies to stabilize signals and separate average and oscillatory components.
The Aron method or two-wattmeter exhibits greater numerical sensitivity and continuous oscillations when reactive power is close to zero, requiring band-stop filtering.

What do these findings contribute?
They provide a simultaneous quantitative evaluation and comparative tool of established power analysis frameworks on a single test platform, ensuring mathematical traceability.
They offer practical advancements for measuring instantaneous power in three-phase systems that lack a neutral conductor through the analytical adaptation of the two-wattmeter method.
They offer guidelines on filtering techniques and numerical stability with logarithmic scales.

Graphical Abstract



doi: 10.25100/iyc.v28i3.16035

Introduction

p - q methods for quantifying instantaneous active-reactive power are a key tool for analyzing power flow and power quality in balanced three-phase systems for smart grids, whether the loads are linear or nonlinear. Commonly applied in the design of active compensators and power filters, *p - q* theory takes the voltages and currents of a three-phase system and transforms them into a two-dimensional orthogonal coordinate system using the transformation (1–8). Furthermore, the Hilbert transform allows for obtaining time-domain representations of the electrical signals to estimate instantaneous active and reactive power. Conventional methods based on RMS values, on the other hand, allow for calculating average power from RMS voltage and current values. When these values are calculated using sliding windows, it is possible to obtain time-domain estimates of average power, although these do not necessarily represent the instantaneous fluctuations within each cycle. These approaches allow for analyzing the energy exchanges between the source and the loads from different perspectives. Under sinusoidal conditions, the average active and reactive power can also be determined by formulating complex power from RMS values, and from the phase shift between voltage and current (1–5,9).

The literature review explores various methods for calculating complex instantaneous power. It is important to distinguish between the mathematical definition of an instantaneous quantity and its practical estimation, since the use of calculation windows, filters, or processing algorithms can introduce time delays. (10). Consequently, the interpretation of the results must consider the temporal characteristics of the estimation procedure, a relevant aspect when comparing the methods analyzed in this study (1,2,13–22,3,23,24,4,5,7–9,11,12).

One of the most widely used theories is the *p-q* theory, which is based on the Clarke transform to decompose instantaneous powers into average and oscillating components (15). Research studies examine non-linear loads, which consist of diode bridge rectifiers. The instantaneous *p-q* theory effectively separates harmonic components and generates reference currents for active filtering (21,25).

Other techniques include the Aron method for three-wire, three-phase systems and the four-wire, three-phase power measurement method. These techniques offer alternatives for measuring power in three-phase systems, depending on the system configuration, within the framework of the IEEE Std 1459-2025 definitions (10). The Aron method for three-wire systems is based on readings from two power measurement elements and can be used as an alternative for power measurement in active filter control strategies (12). This method determines power based on wattmeter readings, without requiring mathematical coordinate transformations of the electrical signals. Meanwhile, the three-phase power measurement method for four-wire systems allows for the determination of total power by measuring the three phases using four wires or via three wattmeters. This method enables the individual assessment of power for each phase and provides comprehensive power information; it is particularly advantageous for systems with non-linear and unbalanced loads, although it does require additional measurement hardware (26).

The choice between these methods depends on the specific application needs and measurement limitations. For example, time-domain analysis excels when working with signals that have harmonic

doi: 10.25100/iyc.v28i3.16035

distortion, transients, or non-sinusoidal elements, which are common in systems powered by electronic power converters (9,13). Furthermore, recent research has pointed out some significant conceptual limitations of this theory when faced with real operating conditions, such as harmonic distortion, voltage imbalances, and nonlinear loads (17,27–29). When ***p-q*** theory is considered as a broader power theory, a fundamental problem arises related to these limitations (27,29).

To mitigate these limitations, several approaches have been proposed. One line of work involves reformulating ***p-q*** theory using alternative mathematical frameworks, such as geometric algebra applied to powers, which allows for a more general analysis and decomposition of instantaneous currents and powers under arbitrary voltage and load conditions. This approach is evaluated on a single-phase RLC load, which entails an increase in computational cost that has not yet been quantified, and the reformulation increases the technical difficulty of its implementation (16). This research proposes to quantify instantaneous active and reactive power, presenting the following contributions:

1. A comprehensive implementation and simultaneous evaluation of three main theoretical frameworks for estimating the instantaneous power of a balanced three-phase system is presented. The methods employed are the Clarke-based ***p-q*** theory, the cross-vector theory combined with the dot-product method, and the time-dependent Hilbert transform.
2. The two-wattmeter method, also known as the Aron method is analytically derived and computationally implemented to calculate the instantaneous active and reactive power components in three-wire systems. This approach offers the advantage of enabling measurements in three-phase systems that lack a neutral conductor.
3. The maximum error, root mean square error, mean absolute error, and absolute and relative errors of each methodology are quantified under various resistive, resistive-inductive, capacitive-resistive, and nonlinear load scenarios. In addition, power values were obtained using proprietary Simscape/Matlab algorithms based on RMS values; these values allowed for comparison of the methods proposed in this study.
4. Methods for calculating instantaneous complex power with and without filtering are analyzed.

This research is organized with the following structure: the second section presents the state of the art, the third section illustrates the development of methods to measure instantaneous power ***p-q***, the fourth section shows the test case, the fifth section presents an analysis of the results, and the sixth section synthesizes the main findings and conclusions of the work.

Literature review

In smart grids, system complexity increases with electronic converters, switched-mode power supplies, and nonlinear loads. Calculating instantaneous power in three-phase systems is an essential tool for analyzing energy flow and power quality, and estimating instantaneous power enables better smart grid operation (22,29–31). The ***p-q*** theory of instantaneous active and reactive power is one of the most widely used approaches for power analysis (5,32). This theory separates active and reactive power components into their fundamental frequency and harmonic components, making it particularly useful for analyzing nonsinusoidal systems in IEEE Std 1459-

doi: 10.25100/iyc.v28i3.16035

2025 (10). However, the ***p - q*** theory has some limitations when the voltage is nonlinear (33). In fact, nonlinear loads present the greatest challenge due to the absorption of nonsinusoidal currents that generate harmonic distortion, affecting the accuracy of conventional metering equipment (32).

The Clarke transform converts balanced three-phase voltages and currents into a two-dimensional αβ coordinate system, simplifying power calculations and providing instantaneous power values (14,15,21,24,33). The general application of the Clarke transform allows for the conversion of voltages and currents from the ABC coordinate system to the stationary αβ0 reference frame. Instantaneous active power is calculated as the dot product of its components (1,7,22–24,34). This theory has been successfully applied in numerous applications. For example, the ***p-q*** theory provides a comparative analysis of shunt active power filters for three-phase, four-wire wye-connected systems, or for compensating harmonics and negative-sequence currents (1,7,8,12,19,29). These phenomena demonstrate that the theory requires preprocessing under certain conditions, especially when dealing with non-ideal network voltages (26,29,33). The literature indicates that the use of the Clarke transform can involve excessive computational effort in certain applications, although it effectively separates homopolar from non-homopolar modes (22,29). Other methods to improve the computational cost have been studied.

The two-wattmeter method was developed by Aron and is a method for measuring power in three-phase, three-wire systems (35). IEEE Std 1459-2025 addresses a three-phase source in a delta connection with a balanced resistive load. This configuration necessitates a formulation for a three-wire delta system that differs from that used for four-wire wye (star) systems. Furthermore, the standard does not evaluate other types of loads (10). The method can be extended to determine the power factor from the ratio of the readings. Its advantage lies in providing an estimate of the RMS values for ***P*** and ***Q*** without requiring a neutral conductor. However, there are no reports on estimating the instantaneous power ***p-q*** (20,35,36). The cross-vector theory and the scalar product method emerge as a vector and scalar alternative to the ***p-q*** model, defining instantaneous reactive power by the cross-product of the voltage and current vectors. This formulation has been described in the literature as equivalent to the ***p-q*** model under certain equilibrium conditions, but with significant differences in the presence of zero sequence or unbalance in four-wire systems composed of three phases and a neutral (18). Complex power has also been studied from two components: 1) active power is associated with the alignment between voltage and current, described by the estimation of the scalar product ***p***, and 2) reactive power represents the energy that is stored and returned to the system; this power is related to the phase shift between voltage and current, which is related to the cross-vector theory ***q***, providing the algebraic basis for the formulation of complex power (19,37).

The Hilbert transform is based on the instantaneous evolution of a signal. This tool has been used to interpret power in the time domain, especially for systems with harmonic and interharmonic components. Recent research proposes signal decomposition methods, for example, using wavelet transforms combined with the Hilbert transform to estimate power quality indices and instantaneous powers of each frequency component, allowing for a more detailed analysis than the classical ***p - q*** method in relation to transients and distortion (9). Another time-evolution-based method is the classical method for calculating power. This method uses RMS values to estimate

doi: 10.25100/iyc.v28i3.16035

voltages and currents with two wattmeters. This technique is widely used in various applications (36). However, research on instantaneous power theories indicates that these RMS methods may not fully capture transient dynamics or significant harmonic content. Despite this, they still serve as a solid reference for average power during steady-state conditions (31,37). One disadvantage of traditional RMS value methods is that they can sometimes underestimate or overestimate power measurements. This is evident when comparing power factor with newer techniques, which can have real consequences for industrial energy metering and billing (31). Furthermore, complex power and its magnitude are derived from RMS voltage and current (20).

The scientific literature review framework compares different power measurement methods that integrate, formulate, and implement instantaneous power and RMS-based power theories, as shown in Table 1. Rather than introducing a completely new theory, this research emphasizes the comparative evaluation and integration of several established approaches, including *p - q* (PQ) theory, cross-vector theory (CVT), and the Hilbert transform (HT). These theories are often examined in isolation with limited combinations (1,7,19,22–24,30,34). The comparison adopts an analysis of mathematical formulations and direct applications in the Matlab/Simulink environment within Simscape, based on RMS values. The methodologies included in Table 1 are classified according to their reproducibility with explicit formulations such as *p-q* theory, cross-vector theory, and the Hilbert transform. These methods are modeled using their equations. This includes the development of analytical matrices and signal-processing blocks, ensuring their mathematical traceability for implementation by third parties.

Furthermore, Simscape blocks are a category corresponding to the native Matlab/Simscape library. The Simscape reference is indicated by (B). This library incorporates internal RMS-based algorithm tools for power calculation, the underlying code of which is not fully accessible due to licensing restrictions. Consequently, Simscape is used as a reference to verify the accuracy of manually implemented explicit formulations. Two hybrid cases are also included. Some implementations combine blocks from the native library with Simscape logic to improve simulation performance and integrate with the methods analyzed by the authors of this study without compromising the integrity of the methods. Within the context of the two-wattmeter (TW) method, also known as the Aron method, it is important to distinguish between formulations based on active power (AP) and reactive power (AQ). It is crucial to clarify that these terms do not imply that the method is limited to calculating only active or reactive power. Both AP and AQ formulations are designed to evaluate the full instantaneous components of active and reactive power. The formulations differ in the algebraic approach used in their derivation. For example, the AP or Aron Simscape *P* formulation comes from the standard sum of wattmeter readings, while the AQ or Aron Simscape *Q* formulation is based on the differential relationship as its main algebraic foundation. The methods discussed are cited in the bibliography along with the Simscape blocks and are relevant to the studies (12,15,26,36).

doi: 10.25100/iyc.v28i3.16035

Table 1. Comparison of power calculation methods and computational implementations.

No	Simscape			HT	TW	PQ	CVT	Reference, first author, year
	B	AP	AQ					
1	No	No	No	No	No	Yes	Yes	(30), Vinifa, 2022
2	No	No	No	No	No	Yes	Yes	(19), Herrera, 2009
3	No	No	No	No	Yes	No	No	(36), Ding, 2011
4	No	No	No	No	No	Yes	Yes	(22), Akagi, 2017
5	Yes	No	No	No	No	Yes	No	(34), Zou, 2023
6	No	No	No	No	No	Yes	Yes	(7), Herrera, 2007
7	No	No	No	No	Yes	No	No	(35), Parton, 1952
8	No	No	No	No	No	Yes	No	(33), Jauhari , 2020
9	No	No	No	No	No	Yes	No	(24), Aguilera, 2024
10	No	No	No	No	No	Yes	No	(32), Van Tung, 2025
11	No	No	No	No	No	Yes	Yes	(11), Peng, 2025
12	No	No	No	Yes	No	No	No	(9), Yu, 2021
13	No	No	No	No	No	Yes	Yes	(18), Akagi, 2001
14	No	No	No	No	No	Yes	No	(37), Beck, 2016
15	No	No	No	No	No	Yes	No	(14), Rajashekaraiah, 2023
16	No	No	No	No	No	Yes	No	(25), Salmerón, 2008
17	No	No	No	No	No	Yes	No	(1), Salmerón, 2009
18	No	No	No	No	No	Yes	Yes	(29), Aredes, 2009
19	No	No	No	No	No	Yes	Yes	(8), Ustariz, 2012
20	No	No	No	No	No	Yes	Yes	(27), Czarnecki, 2014
21	No	No	No	No	No	Yes	No	(2), Tahri, 2005
22	No	No	No	No	No	Yes	Yes	(4), Akagi, 1984
23	No	No	No	No	No	Yes	No	(3), Mikkili, 2011
24	No	No	No	No	No	Yes	No	(5), Satish, 2023
25	No	No	No	No	No	Yes	No	(15), Artemenko, 2024
26	No	No	No	No	No	Yes	No	(12), Artemenko, 2020
27	No	No	No	No	Yes	No	No	(26), Lu, 2022
28	No	No	No	No	No	Yes	No	(21), Kumar, 2024
29	Yes	Yes	Yes	Yes	Yes	Yes	Yes	This comparative study

Note: The nomenclature used is as follows: B denotes the reference case, AP corresponds to the Aron P formulation, AQ corresponds to the Aron Q formulation, HT refers to the Hilbert transform, TW denotes the two-wattmeter method, PQ represents ***p - q theory*** , and CVT denotes the crossed-vector theory.

doi: 10.25100/iyc.v28i3.16035

Unlike previous works that analyze methodologies in isolation or with limited load combinations (12,15,26,36)., this work provides a comparative tool for the simultaneous quantitative evaluation of explicit formulations and those implemented in standard simulation environments. Therefore, this research offers an approach that structures the evaluation of multiple power analysis methods. Studies on instantaneous power are relevant for the development of active power control and filtering applications. The contributions of this research allow for an understanding of the ***p-q*** theory of instantaneous power based on the Clarke transform, as well as the estimation of instantaneous active and reactive power using the two-wattmeter method for balanced three-phase systems. Furthermore, the estimation of instantaneous power through the scalar product and cross-vector theory to determine instantaneous complex power is addressed, finally incorporating a comparative analysis with RMS values.

Instantaneous power for balanced three-phase systems

The first subsection describes the methods and theories for calculating instantaneous complex power. The second subsection presents parameter estimation for a second-order filter that improves the measured power. The third subsection formulates performance indicators based on error metrics.

Methods for estimating instantaneous complex power

All the evaluated methodologies are based on the fundamental assumption of energy conservation in the time domain for balanced three-phase systems with three or four wires. The equivalence between ***p-q*** theory, cross-vector theory combined with the scalar product method, and Aron's method is formulated under balanced sinusoidal conditions. Their extension to nonlinear loads is not straightforward due to the generation of harmonic components, which invalidates the representation of the signals using a single phasor per phase. In nonlinear loads, the harmonic decomposition varies depending on the time frame used, and the phasor relationships obtained cannot be generalized to the non-sinusoidal regime of the signals. The methods for estimating instantaneous complex power are described below.

$$\begin{bmatrix}\mathbf{U}_\alpha\\ \mathbf{U}_\beta\\ \mathbf{U}_0\end{bmatrix}=\begin{bmatrix}\frac{2}{\sqrt{6}} & -\frac{1}{\sqrt{6}} & -\frac{1}{\sqrt{6}}\\ 0 & \frac{1}{\sqrt{2}} & -\frac{1}{\sqrt{2}}\\ \frac{1}{\sqrt{3}} & \frac{1}{\sqrt{3}} & \frac{1}{\sqrt{3}}\end{bmatrix}\begin{bmatrix}\mathbf{U}_A\\ \mathbf{U}_B\\ \mathbf{U}_C\end{bmatrix}=\boldsymbol{K_C}\begin{bmatrix}\mathbf{U}_A\\ \mathbf{U}_B\\ \mathbf{U}_C\end{bmatrix},\mathbf{U}\in\{\mathbf{V},\mathbf{I}\}$$;ystems is (22–24): (1)

Where $\boldsymbol{K_C}$ represents the Clarke matrix, $\mathbf{U}\in\{\mathbf{V},\mathbf{I}\}$ represents the complex number of the current or voltage signal, the substitution $\mathbf{U}_A=U_A\angle 0°$; $\mathbf{U}_B=\mathbf{U}_A\angle -120°$ and $\mathbf{U}_C=\mathbf{U}_A\angle 120°$ are performed for a balanced system.

$$\mathbf{U}_\alpha=\frac{\sqrt{6}}{2}\mathbf{U}_A;\mathbf{U}_\beta=-j\frac{\sqrt{6}}{2}\mathbf{U}_A=-j\mathbf{U}_\alpha,\mathbf{U}\in\{\mathbf{V},\mathbf{I}\}$$ (2)

Where proportionality has been preserved for the time domain, V_m and I_m represent the maximum amplitudes or peak values of the phase voltage and current signals, respectively.

doi: 10.25100/iyc.v28i3.16035

$$v_\alpha(t) = \frac{\sqrt{6}}{2} v_a(t) = \frac{\sqrt{6}}{2} V_m \cos\omega t\,; v_\beta(t) = \frac{\sqrt{6}}{2} V_m \sin\omega t \quad (3)$$

$$i_\alpha(t) = \frac{\sqrt{6}}{2} i_a(t) = \frac{\sqrt{6}}{2} I_m \cos(\omega t - \theta); i_\beta(t) = \frac{\sqrt{6}}{2} I_m \sin(\omega t - \theta) \quad (4)$$

Where θ represents the phase angle between the phase voltage and current, and $\omega = 2\pi f$ denotes the fundamental angular frequency of the system in rad/s. The value of instantaneous active power is defined by (1–8):

$$p_{\alpha\beta}(t) = v_\alpha(t) i_\alpha(t) + v_\beta(t) i_\beta(t) = \frac{3}{2} V_m I_m [\cos\omega t \cos(\omega t - \theta) + \sin\omega t \sin(\omega t - \theta)] \quad (5)$$

In order to simplify the oscillatory terms of the above equation, the trigonometric identity of angle subtraction with cosine is used, where $A = \omega t$ and $B = \omega t - \theta$.

$$\cos(A - B) = \cos A \cos B + \sin A \sin B \quad (6)$$

Therefore, the following equation is obtained, in which the terms dependent on the angular frequency ωt are analytically cancelled $A - B = \theta$. Therefore, under sinusoidal and balanced conditions, the instantaneous active power remains constant over time, fulfilling the following: $p_{\alpha\beta}(t) = p_{\alpha\beta} = P$.

$$p_{\alpha\beta} = \frac{3}{2} V_m I_m \cos\theta = 3 V_{rms} I_{rms} \cos\theta \quad (7)$$

Instantaneous active power $p_{\alpha\beta}(t)$ lacks oscillatory components and is constant over time, numerically coinciding with average active power; this coincides with $P = p_{\alpha\beta}(t)$, because $P = 3 V_{rms} I_{rms} \cos\theta$ given that V_{rms} e I_{rms} denote the effective (rms) phase values of the system, satisfying the relationships that $V_{rms} =$ and $I_{rms} = \frac{I_m}{\sqrt{2}}$. Therefore, under sinusoidal and balanced regime. The reactive power values *q* can be calculated from the following equation (1–8):

$$q_{\alpha\beta}(t) = v_\beta(t) i_\alpha(t) - v_\alpha(t) i_\beta(t) \quad (8)$$

$$q_{\alpha\beta}(t) = \frac{3}{2} V_m I_m [\sin\omega t \cos(\omega t - \theta) - \cos\omega t \sin(\omega t - \theta)] \quad (9)$$

Similarly, the simplification of instantaneous reactive power is carried out using the trigonometric identity of angle subtraction with sine.

$$\sin(A - B) = \sin A \cos B - \cos A \sin B \quad (10)$$

Therefore, under balanced sinusoidal conditions, the instantaneous reactive power component $q_{\alpha\beta}(t)$ exhibits no time variations and is equal in magnitude to the average reactive power Q. Applying identity (10) to Equation (9), the time variable ωt vanishes $A - B = \theta$, demonstrating that the instantaneous reactive power lacks an oscillatory component in balanced regime, so $q_{\alpha\beta}(t) = q_{\alpha\beta} = Q$. Under positive-sequence balanced sinusoidal regime, the oscillatory components

doi: 10.25100/iyc.v28i3.16035

dependent on $2\omega t$ cancel each other analytically ωt, causing the instantaneous active and reactive power to resolve to a time-invariant value that coincides in magnitude with the average power *P* and *Q*. However, oscillatory components may arise in nonlinear loads.

$$q_{\alpha\beta} = \frac{3}{2} V_m I_m \sin\theta = 3 V_{rms} I_{rms} \sin\theta \quad (11)$$

This coincides with $Q = q_{\alpha\beta}(t)$, because $Q = 3V_{rms}I_{rms}\sin\theta$ given that $V_{rms} = \frac{V_m}{\sqrt{2}}$. This method has the advantage that it does not require the use of the neutral to calculate the instantaneous complex power, where $\mathbf{S} = 3\mathbf{V}_A\mathbf{I}_A^* = P + jQ$, $I_{rms} = \frac{I_m}{\sqrt{2}}$ the matrix is obtained.

$$\begin{bmatrix} P \\ Q \end{bmatrix} = \begin{bmatrix} v_\alpha(t) & v_\beta(t) \\ v_\beta(t) & -v_\alpha(t) \end{bmatrix} \begin{bmatrix} i_\alpha(t) \\ i_\beta(t) \end{bmatrix} \quad (12)$$

The Hilbert Transform

The Hilbert transform is $\tilde{v}(t)$ defined as (9):

$$\tilde{x}(t) = \mathcal{H}\{x(t)\} = \frac{1}{\pi}\ \text{p.v.} \int_{-\infty}^{\infty} \frac{x(\tau)}{t-\tau}\, d\tau, x \in \{v, i\} \quad (13)$$

Where p.v. represents the principal Cauchy value and is a convolution with $\frac{1}{\pi t}$. Its 90° offset versions are calculated (9):

$$\tilde{v}(t) = \mathcal{H}\{v(t)\}, \tilde{\imath}(t) = \mathcal{H}\{i(t)\} \quad (14)$$

The formulas are written in their complex signals:

$$\hat{v}_A(t) = v_A(t) + j\,\tilde{v}_A(t), \hat{\imath}_A(t) = i_A(t) + j\,\tilde{\imath}_A(t) \quad (15)$$

Instantaneous complex power $\frac{1}{2}\,\hat{v}_A(t)\,\hat{\imath}_A^*(t)$ is defined as follows:

$$S_A(t) = \frac{1}{2}(v_A(t) + j\,\tilde{v}_A(t))(i_A(t) - j\,\tilde{\imath}_A(t)) \quad (16)$$

Multiply term by term $(v_A(t) + j\,\tilde{v}_A(t))(i_A(t) - j\,\tilde{\imath}_A(t))$:

$$S_A(t) = \frac{1}{2}\,\hat{v}_A(t)\,\hat{\imath}_A^*(t) = \frac{1}{2}(v_A(t) + j\,\tilde{v}_A(t))(i_A(t) - j\,\tilde{\imath}_A(t)) \quad (17)$$

$$S_A(t) = \frac{1}{2}[v_A(t)i_A(t) + j\tilde{v}_A(t)i_A(t) - jv_A(t)\,\tilde{\imath}_A(t) + \tilde{v}_A(t)\,\tilde{\imath}_A(t)] \quad (18)$$

Substituting, we obtain the expression, and by similarity, we calculate expression (1–8):

$$P_A = \frac{V_m I_m}{2}\cos\theta = V_{rms}I_{rms}\cos\theta\,,\ Q_A = \frac{V_m I_m}{2}\sin\theta = V_{rms}I_{rms}\sin\theta \quad (19)$$

Where Q is equal to $3Q_A$ and P is equal to $3P_A$, the matrix summarizes the calculation of the presented expressions.

$$\begin{bmatrix} P \\ Q \end{bmatrix} = \frac{3}{2}\begin{bmatrix} v_A(t) & \tilde{v}_A(t) \\ \tilde{v}_A(t) & -v_A(t) \end{bmatrix} \begin{bmatrix} i_A(t) \\ \tilde{\imath}_A(t) \end{bmatrix} \quad (20)$$

doi: 10.25100/iyc.v28i3.16035

Power using two wattmeters or Aron's method for balanced three-phase systems

The classical Aron method allows the calculation of average active power using two-line measurements. The contribution of this section lies in the analytical derivation of the expression for instantaneous reactive power $q_2(t)$ in the time domain for balanced three-phase systems, defined in Equation (33) and Equation (37). The power calculation using the voltage differential for $\mathbf{V}_{AB}$ and $\mathbf{V}_{CB}$ is presented below, where $\mathbf{V}_A = V_A\angle 0°$; $\mathbf{V}_B = \mathbf{V}_A\angle -120°$; $\mathbf{V}_C = \mathbf{V}_A\angle 120°$ for positive sequence,

these can be calculated using the following expressions (15,26).

$$\mathbf{V}_{AB} = \mathbf{V}_A - \mathbf{V}_B = \sqrt{3}\mathbf{V}_A\angle 30°, \mathbf{V}_{CB} = \mathbf{V}_C - \mathbf{V}_B = \sqrt{3}\mathbf{V}_A\angle 90° \quad (21)$$

Proportionality $\sqrt{3}$ is preserved for the time domain in the following equation.

$$v_{AB}(t) = \sqrt{3}V_m\cos(\omega t + 30°)\,, v_{CB}(t) = \sqrt{3}V_m\cos(\omega t + 90°) \quad (22)$$

Sequences in a balanced system are calculated with the following expressions.

$$\mathbf{I}_A^* = \frac{\mathbf{V}_{AN}^*}{\mathbf{z}_y^*} = \frac{V_A}{Z_y\angle -\theta} = I_A\angle\theta, \mathbf{I}_C^* = \frac{\mathbf{V}_{CN}^*}{\mathbf{z}_y^*} = \frac{V_A\angle -120°}{Z_y\angle -\theta} = I_A\angle(\theta - 120°) \quad (23)$$

The values are analyzed in the time domain, obtaining the following equations.

$$i_A(t) = I_m\cos(\omega t - \theta)\,, i_C(t) = I_m\cos(\omega t - \theta + 120°) \quad (24)$$

The complex power is determined by the following equation.

$$\mathbf{S}_1 = \mathbf{V}_{AB}\mathbf{I}_A^* = \sqrt{3}V_A I_A\angle(\theta + 30°), \mathbf{S}_2 = \mathbf{V}_{CB}\mathbf{I}_C^* = \sqrt{3}V_A I_A\angle(\theta - 30°) \quad (25)$$

Instantaneous power values can be calculated as follows:

$$p(t) = v_{AB}(t)i_A(t) + v_{CB}(t)i_C(t) \quad (26)$$

$$p(t) = \sqrt{3}V_m I_m[\cos(\omega t + 30°)\cos(\omega t - \theta) + \cos(\omega t + 90°)\cos(\omega t - \theta + 120°)] \quad (27)$$

To transform the signal products into summable sinusoidal components, the trigonometric identity for the product of cosines is replaced as shown below:

$$\cos A\cos B = \frac{1}{2}[\cos(A - B) + \cos(A + B)] \quad (28)$$

doi: 10.25100/iyc.v28i3.16035

Substituting the relationship from Equation (28) into the voltage and current expressions of Equation (27), the expanded form of the power flow is obtained.

$$p(t) = \frac{\sqrt{3}V_m I_m}{2}[\cos(30° + \theta) + \cos(2\omega t + 30° - \theta) + \cdots$$

$$\ldots \cos(\theta - 30°) + \cos(2\omega t + 210° - \theta)] \quad (29)$$

The equal terms cancel out and the expression is used,
$\cos(30° + \theta) + \cos(\theta - 30°) = 2\cos\theta\cos 30° = \sqrt{3}cos\theta$, obtaining the following equation. The term ωt has been canceled, so the power is independent of time, therefore $p(t) = P$.

$$P = \frac{3}{2}V_m I_m \cos\theta = 3V_{rms}I_{rms}\cos\theta \quad (30)$$

In the frequency domain, the subtraction is performed between the complex powers calculated for the real component according to the following expressions.

$$P_1 = \sqrt{3}V_{rms}I_{rms}\cos(\theta + 30°), P_2 = \sqrt{3}V_{rms}I_{rms}\cos(\theta - 30°) \quad (31)$$

The active power is obtained from the following expression for each of the two powers (15,26).

$$P = P_1 + P_2 = \sqrt{3}V_{rms}I_{rms}\cos(\theta + 30°) + \sqrt{3}V_{rms}I_{rms}\cos(\theta - 30°) = 3V_{rms}I_{rms}\cos\theta \quad (32)$$

This coincides exactly with $P = p$. Therefore, in a balanced three-phase system in steady state, the instantaneous active power flow $p(t)$ is constant and numerically coincides at every instant with the average active power P. The instantaneous reactive power can be approximated from the following expression.

$$q_2(t) = \sqrt{3} * [v_{CB}(t)i_C(t) - v_{AB}(t)i_A(t)] \quad (33)$$

$$q_2(t) = 3V_m I_m[\cos(\omega t + 90°)\cos(\omega t - \theta + 120°) - \cos(\omega t + 30°)\cos(\omega t - \theta)] \quad (34)$$

The product of cosines is substituted as shown below.

$$q_2(t) = \frac{3V_m I_m}{2}[\cos(\theta - 30°) + \cos(2\omega t + 210° - \theta) \ldots$$

$$\ldots - \cos(\theta + 30°) + \cos(2\omega t + 30° - \theta)] \quad (35)$$

The equal terms are cancelled and the expression
$\cos(\theta - 30°) - \cos(\theta + 30°) = -2\sin\theta\sin -30 = \sin\theta$ is used. The oscillating component is obtained using the following expression.

$$\cos(2\omega t + 210° - \theta) - \cos(2\omega t + 30° - \theta) = -2\sin(2\omega t + 120° - \theta) \quad (36)$$

doi: 10.25100/iyc.v28i3.16035

The expression $q_2(t)$ obtained in Equation (37) contains an average term $\frac{3}{2}V_m I_m \sin\theta$ and an oscillatory term at twice the fundamental frequency $2\omega t$ with a phase shift of $120°$. Eliminating this oscillation using a band-stop filter 120 Hz allows isolating the continuous value equivalent to the steady-state reactive power without losing dynamic tracking during load changes. The instantaneous reactive power is obtained by subtracting the oscillations of the second fundamental component from its average component.

$$q_2(t) = \frac{3}{2}V_m I_m \sin\theta \; - \; 3V_m I_m \sin(2\omega t + 120° - \theta) \qquad (37)$$

The average reactive power is calculated using the RMS power expression (20), where $T = 1/f$ represents the fundamental period of the system's voltage and current signals:

$$Q = \frac{1}{T}\int_0^T q(t)\,dt = \frac{3}{2}V_m I_m \sin\theta = 3V_{rms} I_{rms} \sin\theta \qquad (38)$$

Reactive power is calculated using active power, obtaining the following expression (26).

$$Q = \sqrt{3}(P_2 - P_1) = 3V_{rms} I_{rms}\cos(\theta - 30°) - 3V_{rms} I_{rms}\cos(\theta + 30°)\ldots$$

$$\ldots = 3V_{rms} I_{rms} \sin\theta \qquad (39)$$

The instantaneous current and voltage allow us to arrive at the following matrix in which the average power and instantaneous reactive power are represented.

$$\begin{bmatrix} P \\ q_2(t) \end{bmatrix} = \begin{bmatrix} v_{AB}(t) & v_{CB}(t) \\ -\sqrt{3}v_{AB}(t) & \sqrt{3}v_{CB}(t) \end{bmatrix} \begin{bmatrix} i_A(t) \\ i_C(t) \end{bmatrix} \qquad (40)$$

Dot product p **and crossed vector theory** q

The dot product $p(t) = \vec{i}(t) \cdot \vec{v}(t)$ is represented by the following equations; the vectors represent the three-phase instantaneous current $\vec{i}(t) = i_A(t)\hat{\imath} + i_B(t)\hat{\jmath} + i_C(t)\hat{k}$ and the three-phase instantaneous voltage $\vec{v}(t) = v_A(t)\hat{\imath} + v_B(t)\hat{\jmath} + v_C(t)\hat{k}$ (17,26). The three-phase variable is composed of phases A , B and C.

$$p(t) = i_A(t) \cdot v_A(t) + i_B(t) \cdot v_B(t) + i_C(t) \cdot v_C(t) \qquad (41)$$

$$p(t) = I_m V_m[\cos\omega t \cos(\omega t - \theta) + \cos(\omega t - 120°)\cos(\omega t - \theta - 120°)\ldots$$

$$\ldots + \cos(\omega t + 120°)\cos(\omega t - \theta + 120°)] \qquad (42)$$

The terms are simplified to the following expression by applying the trigonometric identity.

$$p(t) = \frac{I_m V_m}{2}[\cos\theta + \cos(2\omega t - \theta) + \cos\theta + \cos(2\omega t - \theta - 240°)\ldots$$

$$\ldots + \cos\theta + \cos(2\omega t - \theta + 240°)] \qquad (43)$$

doi: 10.25100/iyc.v28i3.16035

The terms are grouped and added together. Instantaneous active power is independent of time $p(t) = P$ therefore, the expressions are reduced to the following equation.

$$P = \frac{3}{2} I_m V_m \cos\theta = 3 V_{rms} I_{rms} \cos\theta \quad (44)$$

The vector product $\vec{q}(t) = \vec{i}(t) \times \vec{v}(t)$ is represented by the determinant using the unit vectors $\hat{i}, \hat{j}$ on $\hat{k}$ each axis

$$\vec{q}(t) = \begin{bmatrix} \hat{i} & \hat{j} & \hat{k} \\ i_A(t) & i_B(t) & i_C(t) \\ v_A(t) & v_B(t) & v_C(t) \end{bmatrix} \quad (45)$$

The system is symmetrical $q_{\hat{i}}(t) = q_{\hat{j}}(t) = q_{\hat{k}}(t)$**.** Therefore, the magnitude of q for the system it is:

$$Q = \sqrt{Q_{\hat{i}}^2 + Q_{\hat{j}}^2 + Q_{\hat{k}}^2} = 3 V_{rms} I_{rms} \sin\theta \quad (46)$$

In the time domain, the estimation of instantaneous reactive power is performed using the phase extractor oriented on the axis component $\hat{j}$. Given the symmetry of the balanced three-phase system $q_{\hat{i}}(t) = q_{\hat{j}}(t) = q_{\hat{k}}(t)$, the total instantaneous reactive power scalar signal $q(t)$ is determined by scaling the extracted component by the factor $\sqrt{3}$.

$$q(t) = \sqrt{3} q_{\hat{j}}(t) = \sqrt{3} * [i_C(t) v_A(t) - i_A(t) v_C(t)] \quad (47)$$

By replacing the time-domain sinusoidal signals in the previous equation, the time-domain substitutions are obtained, resulting in the following equation.

$$q(t) = \sqrt{3} I_m V_m [\cos(\omega t - \theta + 120°) \cos\omega t - \cos(\omega t - \theta) \cos(\omega t + 120°)] \quad (48)$$

The angle sum identity is applied to the expression, yielding the following result:

$$q(t) = \frac{\sqrt{3} I_m V_m}{2} [\cos(-\theta + 120°) + \cos(2\omega t - \theta + 120°) \ldots$$
$$\ldots - \cos(-\theta - 120°) - \cos(2\omega t - \theta + 120°)] \quad (49)$$

Since the oscillatory components dependent on ωt cancel each other out due to the symmetry of the three-phase system, the values reduce to the following expression, because the instantaneous reactive power is independent of time q (t) = Q, and is given by the following expression.

$$Q = \frac{\sqrt{3} I_m V_m}{2} [\cos(-\theta + 120°) - \cos(-\theta - 120°)] \quad (50)$$

This expression is used $\cos(-\theta + 120°) - \cos(-\theta - 120°) = 2 \sin\theta \sin 120°$ to determine the value of the instantaneous reactive power.

doi: 10.25100/iyc.v28i3.16035

$$Q = \frac{3}{2} I_m V_m \sin\theta = 3 V_{rms} I_{rms} \sin\theta \quad (51)$$

Design of a second-order filter

Two types of filters are designed to improve the output signal of the active and reactive power.

Design of a low-pass filter

The filter's design parameters are configured to allow the passage of frequencies below 5 Hz and a damping factor of $\zeta = 0.707$, characterized by a maximally flat frequency response in the passband and a minimum time-domain overshoot of 4.32% for step input, making it suitable for applications requiring a stable response without significant distortion in the time domain. The value of ζ corresponds to a Butterworth response characterized by a smooth transition. The natural angular frequency ω_n is obtained from the natural frequency using the relationship $\omega_n = 2\pi f_n$, substituting the value of f_n equal to $\omega_n = 2\pi(5) = 10\pi \approx 31.42$ rad/s. The transfer function of a second-order low-pass filter allows substituting the calculated parameters $\omega_n^2 = 986.96$ and $2\zeta\omega_n = 44.43$. The system's transfer function is finally defined as:

$$F_{lp}(s) = \frac{\omega_n^2}{s^2 + 2\zeta\omega_n s + \omega_n^2}; F_{lp}(s) = \frac{986.96}{s^2 + 44.43s + 986.96} \quad (52)$$

Where s represents the complex frequency variable in the Laplace transform domain.

Design of a band-reject filter

The filter is defined by the parameters 1) the second fundamental harmonic is $f_n = 120$ Hz , and 2) the damping factor is $\zeta = 0.15$. This generates more selective rejection, i.e., a narrower band. The selection of these parameters allows the suppression of specific 120 Hz frequency components without significantly affecting the rest of the spectrum. The natural angular frequency ω_n is determined by $\omega_n = 2\pi f_n$. Substituting the value of the center frequency equal to $\omega_n = 2\pi(120) = 240\pi \approx 753.98$ rad/s. The transfer function of a second-order band-stop filter allows selective attenuation of a narrow range of frequencies around ω_n. By substituting the obtained values $\omega_n^2 \approx 568493$ and $2\zeta\omega_n \approx 226.19$, the filter's transfer function is defined as:

$$F_{bs}(s) = \frac{s^2 + \omega_n^2}{s^2 + 2\zeta\omega_n s + \omega_n^2}; F_{bs}(s) = \frac{s^2 + 568493}{s^2 + 226.19s + 568493} \quad (53)$$

Performance indicators

Performance indicators are based on error metrics that are described below.

a. Calculation of the absolute error

The absolute error is calculated by subtracting M_{method} the true power from the estimated power for each method, as presented in the equation.

$$\epsilon_a(t) = | M_{method}(t) - M_{ref}(t) |, M \in \{P, Q\} \quad (54)$$

b. Calculation of the relative error

doi: 10.25100/iyc.v28i3.16035

The relative error is calculated by dividing the absolute error by the true power or reference power at each instant in time. For the case of Q in a resistive load with Q_{ref}= 0, the relative error is not reported to avoid divisions by zero.

$$\epsilon_r(t) = \frac{\epsilon_a(t)}{M_{ref}(t)} = \frac{|M_{method}(t) - M_{ref}(t)|}{M_{ref}(t)}, M \in \{P, Q\} \quad (55)$$

c. Calculation of the maximum error

The maximum error is calculated by subtracting the maximum power recorded over an interval of each load from the deviation from the reference and N represents the number of samples in the analyzed load interval.

$$\epsilon_{\max} = \max_{k \in \{1,\ldots,N\}} |M_{method}(k) - M_{\text{ref}}(k)|, \quad M \in \{P, Q\} \quad (56)$$

d. Calculation of the average absolute error

The mean absolute error (MAE) is estimated by subtracting the estimated power for each method from the true power for the analyzed load range.

$$\text{MAE} = \frac{1}{N}\sum_{k=1}^{N} |M_{method}(k) - M_{\text{ref}}(k)|, M \in \{P, Q\} \quad (57)$$

e. Calculation of the root mean square error

The root mean square error (RMSE) allows us to estimate the squared difference of the power estimated for each method for the analyzed load range.

$$\text{RMSE} = \sqrt{\frac{1}{N}\sum_{k=1}^{N} \left(M_{method}(k) - M_{\text{ref}}(k)\right)^2}, M \in \{P, Q\} \quad (58)$$

f. Calculation of the percentage overshoot

The percentage overshoot (M_p) is the maximum excess of the transient response over the steady-state value, expressed as a percentage.

$$M_p(\%) = \frac{M_{\max} - M_{\text{ref}}}{|M_{\text{ref}}|} \times 100, M \in \{P, Q\} \quad (59)$$

Test case

In Figure 1, the balanced three-phase circuit consists of three phases with uniformly distributed loads, resulting in equal impedances in each phase. The interconnection of the elements is presented in a symmetrical configuration, where the phase voltages are equal at 120 V_{rms} at 60 Hz and are 120° out of phase with each other. The dashed lines represent the source and load blocks associated with each phase, highlighting the structural repetition characteristic of a balanced system. The common ground and neutral reference point is also shown, allowing for analysis of current and voltage behavior in the system. Three-phase systems are characterized by the fact that the sum of the currents flowing through the neutral conductor is equal to zero when the loads are balanced. This configuration is used because it improves the stability of electrical power transmission and distribution. The balanced three-phase electrical circuit with load phase control is shown in Figure 2. For computational simulation in the MATLAB/Simulink environment with

doi: 10.25100/iyc.v28i3.16035

Simscape, a variable-step solver with relative tolerance $10^{-3}$and automatic absolute tolerance was configured, executed over a range of 0 s to 4 s with an adaptive integration step. The loads are connected in a four-wire star configuration **A**, **B**, **C**, and **N,** and are switched by means of solid-state switches at 1 s intervals. The filters were implemented in the continuous Laplace domain using transfer function blocks with zero initial state conditions $x(0) = 0$. The system is powered by three sinusoidal voltage sources ($\mathbf{V_A}$, $\mathbf{V_B}$, $\mathbf{V_C}$) phase-shifted by 120° from each other and referenced to a common neutral (**N**), configuring a four-wire three-phase system. Each phase (**A**, **B** and **C**) feeds a set of distributed loads, represented by equivalent impedances $\mathbf{Z}_{L_A}$, $\mathbf{Z}_{LB}$ and $\mathbf{Z}_{LC}$. The resistive load is equal to 25 Ω, the resistive-inductive load is equal to 25 Ω + j113.1 Ω, the inductance being equal to 0.3 H, and the resistive-capacitive load is equal to 37 - j24.86 Ω, with the capacitance being equal to 106.7 μF. These loads are organized into electronically controlled branches using solid-state switches, which allow for selective load connection and disconnection. The diagram shows load control blocks for each phase, where resistive and inductive branches can be discretely activated, as well as the nonlinear load based on a universal bridge AC-DC converter, which feeds an RL load on the DC link. Electronic switching modules for dynamic control of phase currents ($\mathbf{I_A}$, $\mathbf{I_B}$, $\mathbf{I_C}$) are also included. Dashed lines delineate functional sections of the system, such as the three-phase power supply area and the load control blocks.

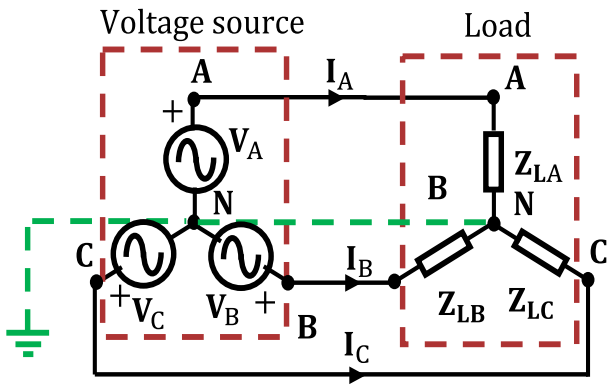


Figure 1. Balanced three-phase circuit

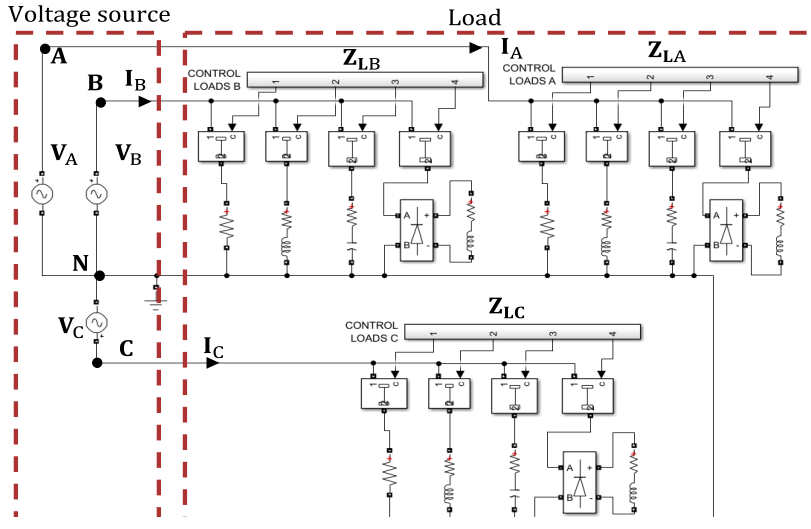


Figure 2. Representation of a balanced three-phase circuit

doi: 10.25100/iyc.v28i3.16035

A balanced three-phase electrical system is connected using the two-wattmeter power measurement method, labeled W_1 and W_2, as shown in Figure 3. The diagram shows a three-phase source supplying a balanced load, represented by red dashed blocks, indicating the system's symmetry. The connection of the three system lines is shown at the bottom of the diagram, where the phase conductors are clearly distinguished. Voltage measurements are taken using two wattmeters connected to two of the lines, while the third serves as a common reference. Wattmeter W_1 is connected between phases A and B and the system reference line. This instrument measures the power corresponding to that specific combination of current and voltage. The wattmeter W_2 is connected between phases B and C and the same reference line. This instrument provides a second, independent reading of the system's partial power. The two wattmeters are connected to two separate lines of the three-phase system, and their voltage coils are connected to the common third line. This configuration corresponds to Aron's method for power measurement in three-wire systems. Figure 4 presents the Simulink, Matlab/Simscape implementation of a power measurement system based on three-phase electrical signal processing, structured using functional blocks for acquisition, calculation, and digital filtering. The model's input stage considers the system's electrical variables, specifically the line voltages and currents. Although the diagram shows three voltages labeled as $\mathbf{V_A}$,$\mathbf{V_B}$ and $\mathbf{V_C}$, the system operates internally with line voltages, the inputs being $\mathbf{V_{AB}}$ and $\mathbf{V_{BC}}$. These signals are processed within the measurement block, which reconstructs the phase variables through internal subtraction operations between the line signals, thereby obtaining the quantities required to calculate active and reactive power. Subsequently, the voltage and current signals v_a, v_b, v_c, i_a, and i_c are fed into the central block, designated as 2W, which implements an algorithm equivalent to the two-wattmeter method. This block generates the active power signals p and reactive power q, corresponding to the instantaneous processing of the electrical variables. The output signals from the 2W block undergo a conditioning process using low-pass filters, which smooth the power components and reduce high-frequency fluctuations associated with switching noise. Furthermore, a more selective filtering stage is implemented for the reactive power signal using a band-reject filter, designed to attenuate the component corresponding to the second harmonic of the fundamental frequency, ensuring a more stable signal estimate q.

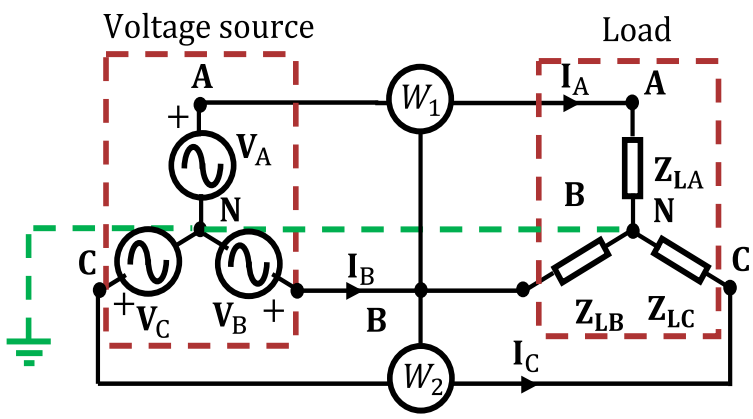


Figure 3. Measurement with two wattmeters

doi: 10.25100/iyc.v28i3.16035

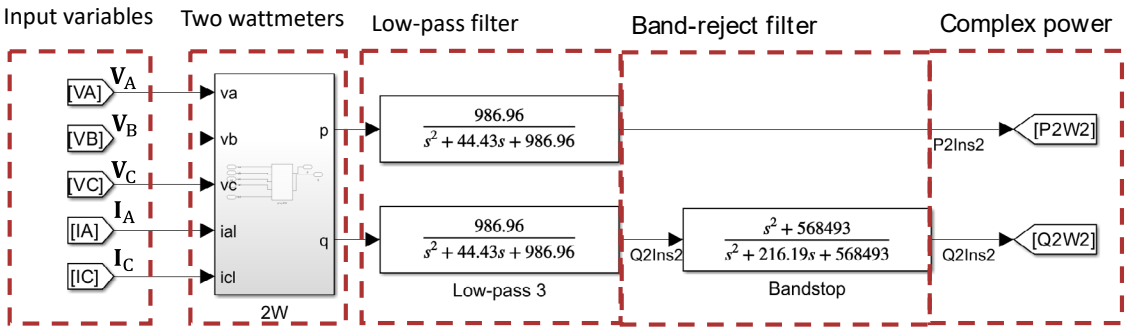


Figure 4. Simulation with two wattmeters

The architecture of a three-phase power estimation system is implemented in the Simulink/Matlab environment; the design is made to calculate active and reactive power from phase voltage and current, as shown in Figure 5. The input stage considers the three-phase voltage signals $\mathbf{V_A}$, $\mathbf{V_B}$,$\mathbf{V_C}$ and current $\mathbf{I_A}$, $\mathbf{I_B}$ and $\mathbf{I_C}$ as measured variables of the electrical system. These signals are processed in the methods block. The same measurement block is applicable with any of these three methods: 1) *p-q* theory or 2) scalar product *p* and cross vector *q*. The calculation of instantaneous power for any of the three methods is performed using a low-pass filter to produce the complex power comprising: 1) instantaneous active power, denoted *p*, and 2) instantaneous reactive power, denoted *q*. These values are determined using algebraic functions of the phase voltages and currents. This process allows obtaining smoothed *p* and *q* signals. Figure 6 presents the scheme for estimating instantaneous active and reactive power from voltage and current signals in the time domain. The system receives as inputs the voltage $\mathbf{V_A}$ and the current $\mathbf{I_A}$ corresponding to one phase of the electrical system under analysis. These signals are applied to a power calculation block, which derives the instantaneous active power component $p(t)$ and the instantaneous reactive power component $q(t)$. The measurement scheme applies two methods: the Hilbert transform and the Simscape power block. Based on RMS values. After extracting representative power values, both signals are processed using second-order low-pass filters. These filters allow for the preservation of low-frequency components.

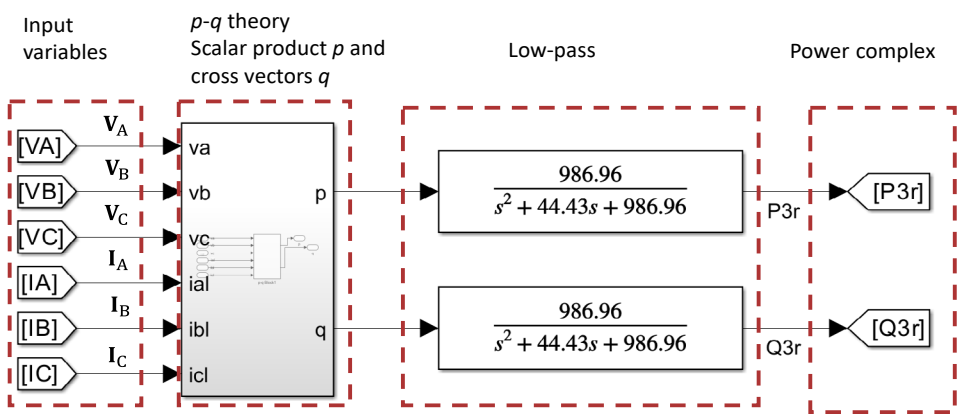


Figure 5. Simulation with three wattmeters

doi: 10.25100/iyc.v28i3.16035

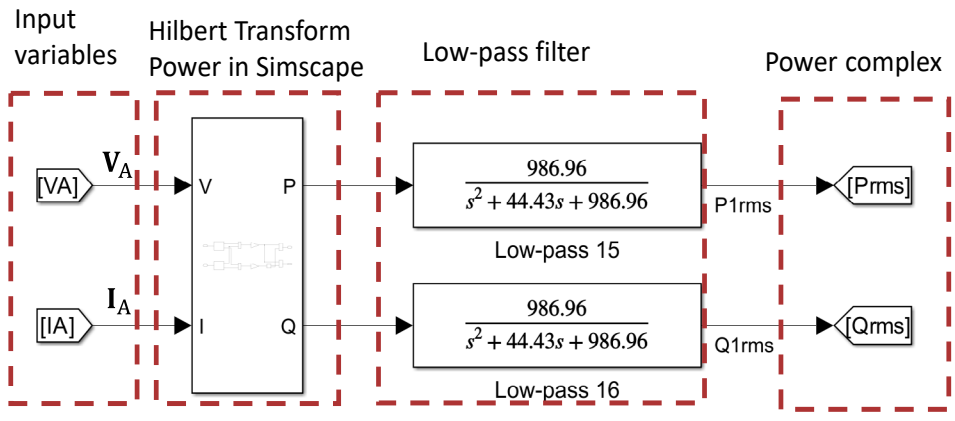


Figure 6. Simulation with a wattmeter

Furthermore, the case study examines two methods that can be applied as a reference. The first will be called the Aron Simscape *P* method and the second, the Aron Simscape *Q* method. The first was calculated in the section on power using two wattmeters, or the Aron method for balanced three-phase systems, and the second is calculated from the following expressions. Reactive and active power are calculated as follows:

$$Q = Q_2 + Q_1 = 3\,V_{rms} I_{rms} \sin\theta ; P = \sqrt{3}(Q_1 - Q_2) = 3\,V_{rms} I_{rms} \cos\theta \quad (60)$$

Where Q_1 and Q_2 correspond to the reactive power components associated with the individual measurements of the first and second wattmeters in the Aron configuration. Figure 7 presents the MATLAB Simulink implementation with Simscape of the two-wattmeter method, also known as the Aron method, for power estimation in three-phase systems. The model integrates two complementary approaches: the calculation of active power *P* and reactive power *Q*, denoted in the diagram as Aron Simscape *P* and Aron Simscape *Q*, respectively. The system receives as inputs the instantaneous voltage and current signals corresponding to two phases of the three-phase system: $\mathbf{V_{AB}}$, $\mathbf{V_{CB}}$, $\mathbf{I_A}$ and $\mathbf{I_C}$. These signals feed two main blocks representing the two wattmeters of the Aron method. Each block performs the instantaneous product of voltage and current, thus generating the instantaneous powers P_1 and P_2, and their corresponding reactive components Q_1 and Q_2. The central section of the diagram implements the algebraic processing characteristic of the two methods. To estimate the total active power, the contributions of both wattmeters are summed, followed by scaling by a factor $1/3$, to obtain the power for one phase.

doi: 10.25100/iyc.v28i3.16035

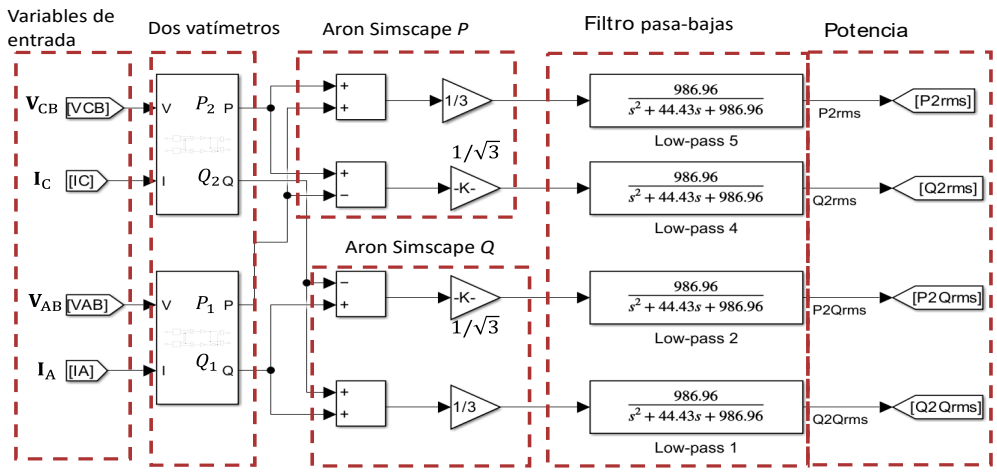


Figure 7. Simscape reference with 2 wattmeters.

On the other hand, for reactive power, $1/\sqrt{3}$ is a linear combination based on the difference between the terms together with a scaling factor, to obtain the power of a phase. These operations correspond to the analytical expressions derived from the two-wattmeter method for balanced systems. Subsequently, the signals are filtered using second-order low-pass filters, which allow the active and reactive powers to be obtained by eliminating the high-frequency oscillatory components present in the instantaneous signals. Furthermore, the complex power of the outputs is provided with the magnitudes $P_{2,\mathrm{rms}}$ and $Q_{2,\mathrm{rms}}$, which represent the smoothed estimates of the active and reactive power of the balanced three-phase system.

Table 2 presents a comparison of different methods used to measure and analyze electrical power in balanced three-phase systems, considering the number of wattmeters required, the need for filtering, and the type of electrical system in which they are applied. Measurements with one wattmeter employ methods such as the Simscape-based reference and the Hilbert transform, which can measure both single-phase and balanced three-phase systems.

Table 2. Methods for measuring active and reactive power.

No	Methods	Watt-meters	Low-pass filter	Band-reject filter	System
1	Simscape Reference	1	Yes	No	Single-phase; Balanced three-phase
2	Hilbert Transform	1	Yes	No	Single-phase; Balanced three-phase
3	Aron or two wattmeters	2	Yes	Yes	Balanced three-phase
4	Aron Simscape *P*	2	Yes	No	Balanced three-phase
5	Aron Simscape *Q*	2	Yes	No	Balanced three-phase
6	*p-q* theory	3	Yes	No	Balanced three-phase
7	CVT	3	Yes	No	Balanced three-phase

doi: 10.25100/iyc.v28i3.16035

Measurements with two wattmeters are distinguished by the use of three methods: 1) the Aron method or two-wattmeter method, 2) the Aron Simscape *P* method and 3) Aron Simscape's method *Q*. Method 1 requires two wattmeters and the combined use of a low-pass filter and a band-stop filter. The former allows for obtaining average power values, while the latter facilitates the elimination of specific harmonic components, improving accuracy under non-ideal conditions. For measurements with three wattmeters for balanced three-phase systems, theories based on instantaneous power are used, such as *p-q* theory, the dot product method, and the cross-vector theory. All methodologies employ low-pass filters to separate the average active and reactive power components.

Results

The methods studied are designed for calculating active and reactive power in linear loads. Therefore, their application to nonlinear loads requires further evaluation, as their validity under these conditions has not been established. For this evaluation, the Simscape/MATLAB power measurement block, a commercial tool whose behavior is used as a benchmark for comparison, is used as a reference. Active and reactive power values are obtained once the steady-state regime is reached after switching. Because information on the block's internal implementation is unavailable, the obtained values are considered comparative benchmarks rather than exact theoretical values. Based on these values, the deviation of the proposed method's results from the software benchmark is quantified, without assuming its validity for nonlinear loads beforehand. Furthermore, Aron Simscape *P* and Aron Simscape *Q* are not methods exclusively for calculating active or reactive power, but rather two formulations based on wattmeter readings from the Aron method. The algebraic sum or difference of *P*/*Q* is used to determine active or reactive power. Both components allow for obtaining the complex power $\boldsymbol{S} = P + jQ$. These formulations are presented in Equation (32) and Equation (60), respectively.

The absolute error of the active power is evaluated with four types of loads: resistive, resistive-inductive, resistive-capacitive, and nonlinear. The seven methods switch their loads as shown in Table 2 and Figure 8. The logarithmic scale is used because it facilitates the visualization of results close to zero. The maximum absolute error values of 576 W, 548.89 W, 241.29 W, and 1457.89 W are displayed for the four switching operations at times around 0 s, 1 s, 2 s, and 3 s, respectively. After each switching operation, the absolute error of all seven calculation methods decreases rapidly. The four loads are evaluated after 0.33 s, and the absolute errors drop to 0.6 W, 0.59 W, 0.2 W, and 0.55 W at approximately 0.33 s, 1.33 s, 2.33 s, and 3.33 s, respectively. After these times, the absolute errors of the active power continue to decrease. At the end of each switching cycle, absolute error valleys are detected, falling around 3.41×10^{-13}W, 1.41×10^{-8}W, 1.36×10^{-9}W, and 8.96×10^{-10}W. The minimum absolute errors are 6.92×10^{-4}W, 4.81×10^{-5}W, 2.9×10^{-4}W for the resistive, resistive-inductive, and resistive-capacitive loads, respectively. Furthermore, the minimum error in the nonlinear load does not stabilize and oscillates between a range of 3.17×10^{-7}W to 3.59×10^{-2}W. A noticeable difference appears in the method based on the Hilbert transform. Although it follows a similar trend to the other methodologies, it exhibits a higher level of absolute error than the other six methods after 0.6 s of each switching cycle. The greatest divergence

doi: 10.25100/iyc.v28i3.16035

between methodologies is observed during operation with non-linear loads; this behavior is expected because the methods developed in this research are formulated for resistive, capacitive, and inductive loads.

In nonlinear loads, the reference active power (P_{ref}) is defined as the constant value reached once stabilization is achieved. The Simscape active power block is based on RMS values; it is used as a reference for the other methods; its underlying code is not fully accessible due to licensing restrictions. Furthermore, this research presents hybrid methods that combine Simscape methods and formulations presented herein, such as the Aron Simscape *P* method and the Aron Simscape *Q* method, which are based on RMS values presented in Equation (32) and Equation (60). In the nonlinear load region, persistent oscillations and a more pronounced dispersion between the curves appear. The two-wattmeter method exhibits the highest absolute errors and sustained oscillation throughout the analyzed interval, while the methods based on *p-q* theories, the dot product *P*, and Aron implementations maintain lower errors.

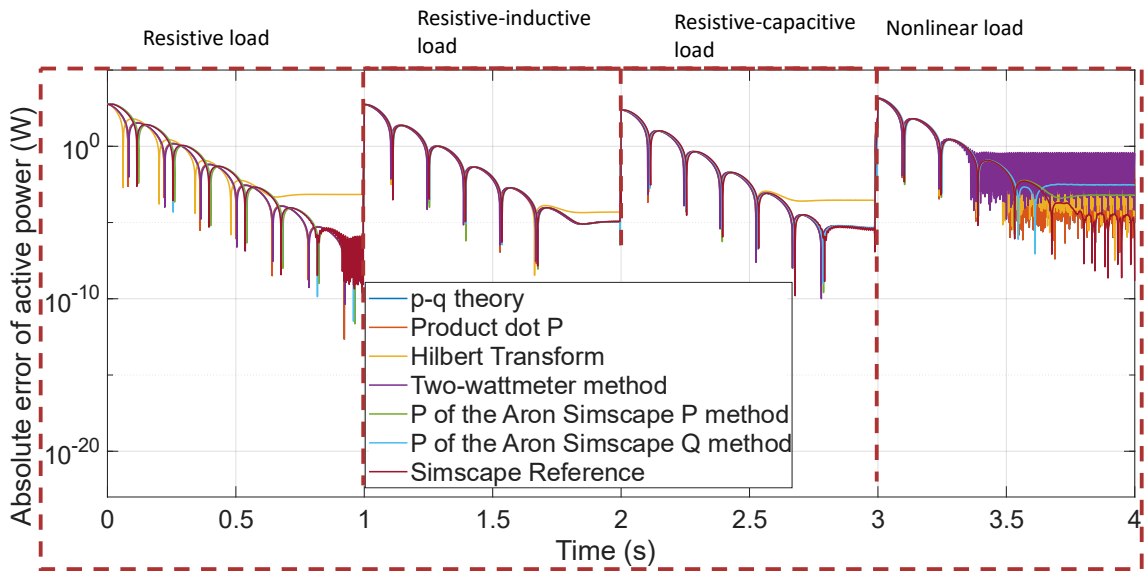


Figure 8. Absolute error of active power.

Figure 9 presents the time evolution of the absolute reactive power error for seven estimation methods, evaluated under four load types: 1) resistive, 2) resistive-inductive, 3) resistive-capacitive, and 4) nonlinear. The vertical axis is represented on a logarithmic scale to facilitate the comparison of errors spanning several orders of magnitude of reactive power in VAR and to allow the visualization of values close to zero. The maximum absolute errors recorded were 35.65 VAR, 121 VAR, 301.7 VAR, and 574.26 VAR for the resistive, resistive-inductive, resistive-capacitive, and nonlinear loads, respectively. The absolute errors drop drastically to 0.23 VAR, 0.092 VAR, 0.25 VAR, and 0.3 VAR at approximate times of 0.33 s, 1.33 s, 2.33 s, and 3.33 s, respectively. Furthermore, the absolute errors exhibit minimum values of 1.92×10^{-12} VAR, 4.08×10^{-10} VAR, 7.82×10^{-12} VAR and 4.1×10^{-9} VAR for resistive, resistive-inductive, resistive-capacitive, and nonlinear loads, respectively. The Hilbert transform exhibits a response with a limiting absolute error that is higher than the other six methods after 0.6 s. The Simscape reactive power block based on RMS values is used as a reference for the other methods. In addition, this research presents hybrid methods that combine Simscape methods and reactive formulations, such as the Aron Simscape

doi: 10.25100/iyc.v28i3.16035

P method and the Aron Simscape *Q* method, which exhibit values close to the reference. The curves corresponding to the ***p-q*** and cross-product theory remain practically overlapping and with oscillations of absolute error. The nonlinear load region shows an increase in the value of the oscillations for all seven methods; the Simscape reference methods based on RMS values show a lower scattering frequency and achieve lower absolute errors.

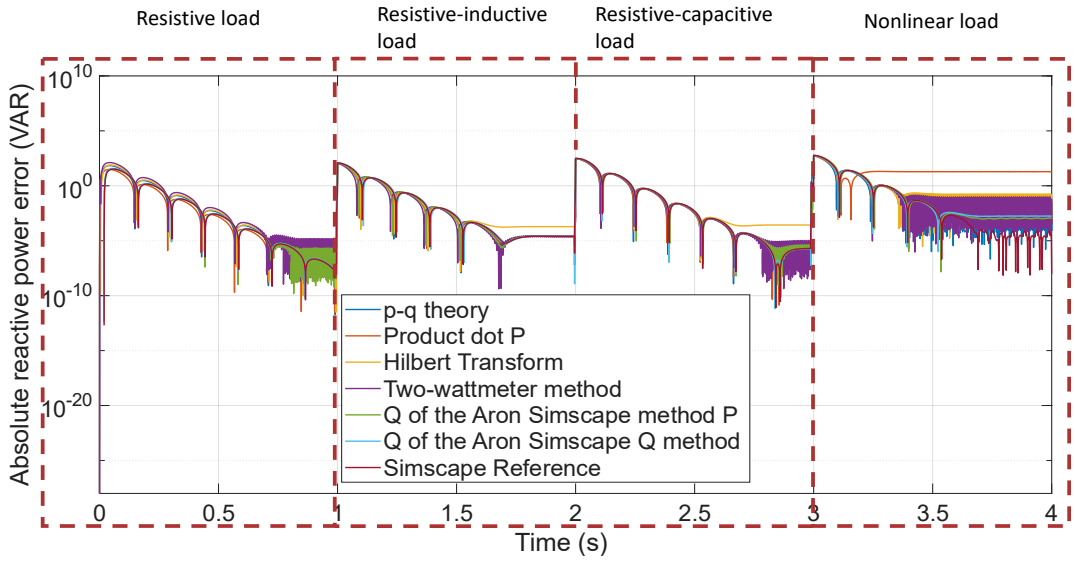


Figure 9. Absolute error of reactive power.

Figure 10 presents the time evolution of the relative error of the active power for the seven estimation methods. The oscillations coincide with those shown for the absolute error of the active power. The time evolution of the relative error of the active power is expressed on a logarithmic scale and lasts from 0 to 4 s. The simulation interval is divided into four operating regions: 1) resistive load, 2) resistive-inductive load, 3) resistive-capacitive load, and 4) nonlinear load. The initial value of the seven methods is significantly different from the reference solution, with values of 1) 99%, 2) 2008%, 3) 89.9%, and 4) 81% for each region, respectively. The methods converge rapidly to viable solutions with an error of less than 1% in times of 1) 0.22 s, 2) 0.34 s, 3) 0.2 s, and 4) 0.177 s, respectively. The seven methods are compared; the Hilbert transform has the highest relative error, and the *P* estimation using the Aron Simscape *Q* method has the highest relative error for nonlinear loads. In both cases, the relative error reaches approximately 1.7×10^{-4}% without oscillations. For nonlinear loads, the two-wattmeter method exhibits large oscillations ranging between 0.022% and 3.63×10^{-6}%. The lowest relative errors are reported between 10^{-8} and 10^{-14} which are obtained by the Simscape and dot product methods.

doi: 10.25100/iyc.v28i3.16035

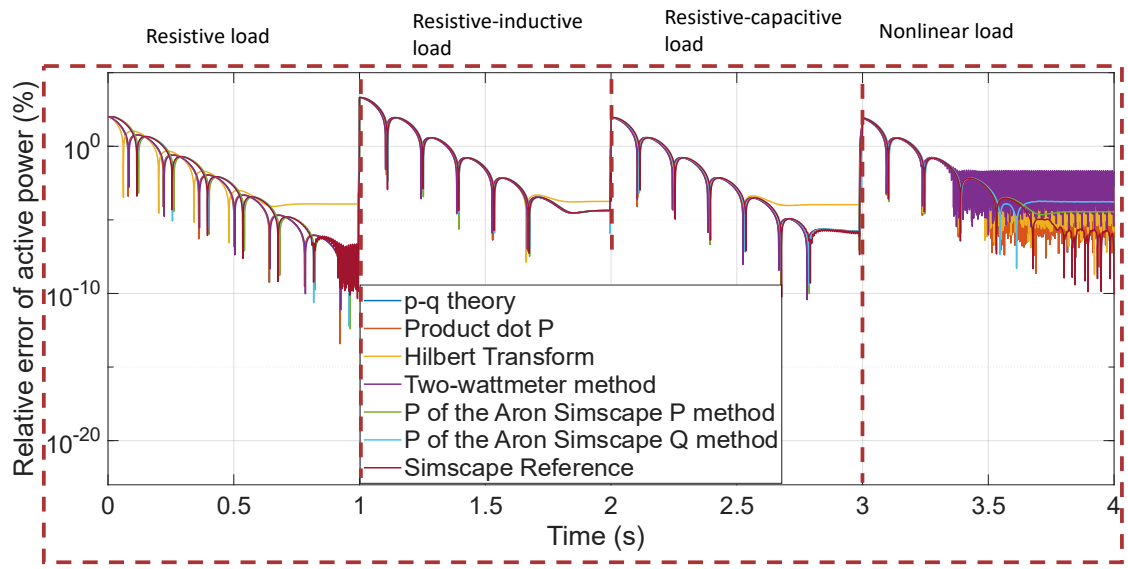


Figure 10. Relative error of active power.

The relative error of reactive power is presented as a function of time for the seven estimation methodologies, as shown in Figure 11. The relative error axis is expressed on a logarithmic scale for the different methodologies considered, and the evaluation is performed over 4 seconds. In the evaluation of the relative error of reactive power, the resistive load is excluded because $Q_{ref} = 0$ VAR generates an indeterminacy due to division by zero. The two-wattmeter method exhibits error oscillations around $10^{-5}\%$ for resistive-inductive loads, resistive-capacitive loads, and nonlinear loads, oscillations reach the range between10^{-6} and $10^{-9}\%$ in the resistive capacitive load and the oscillations for the nonlinear load reach the interval between 10^{-6} and $10^{-9}\%$ for nonlinear loading.

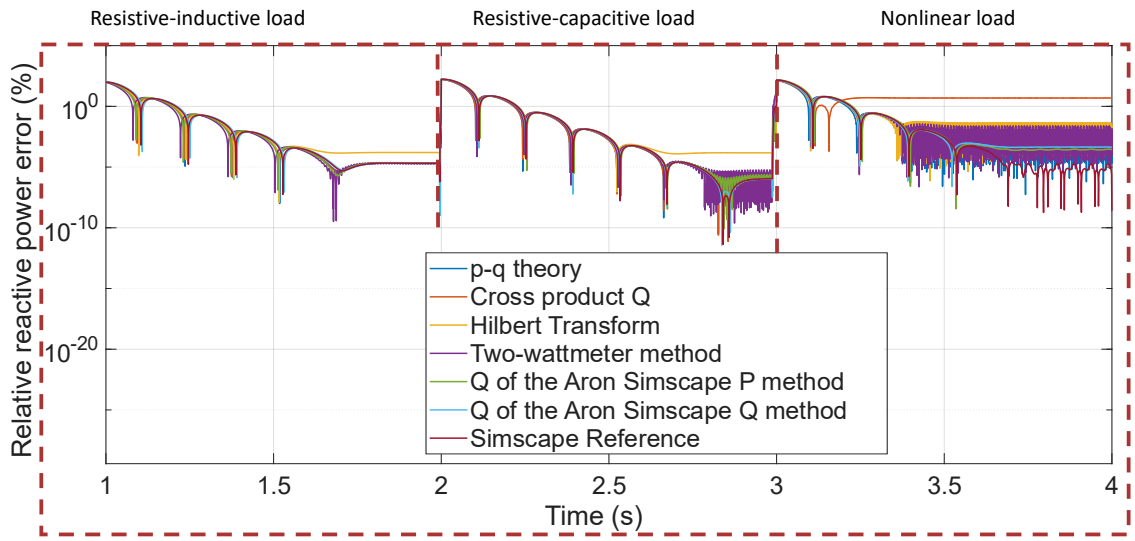


Figure 11. Relative error of reactive power.

doi: 10.25100/iyc.v28i3.16035

The reactive power of the Aron Simscape *Q* method exhibits low oscillations for resistive-inductive loads, around $1.7 \times 10^{-6}\%$, and for nonlinear loads, the relative error oscillations are less frequent, around $2.6 \times 10^{-4}\%$, close to the *p-q* theory, which shows low oscillations of $4.2 \times 10^{-4}\%$. For nonlinear loads, the dot product shows the highest relative error of the reactive power, around 4.89%, followed by the Hilbert transform, oscillating in a range between 0.045% and 3.24%. The Hilbert transform has the highest relative error, reaching values of $1.5 \times 10^{-4}\%$ for resistive-inductive and resistive-capacitive loads.

The filtered and unfiltered methods in Figure 12 follow an active power reference. Active power is represented by dashed lines for unfiltered power and solid lines for filtered power. Unfiltered active power exhibits an overshoot of 2570 W, 295.4 W, and 2026.29 W for resistive, resistive-capacitive, and nonlinear loads, respectively, and exhibits a negative overshoot of -34.71 W for the resistive-inductive load. The Hilbert transform shows the highest overshoots, followed by the dot product and *p-q* theory for the analyzed loads. At the end of the simulation for the nonlinear load, these methods maintain constant oscillations. The methods based on the Simscape reference have lower overshoots and require a waiting period of 0.0167 s to obtain the first result. The Simscape RMS methods have a slower response time than the other methods. Oscillations are reduced for all loads, most noticeably for the nonlinear load, where the solution stabilizes. The study methods are formulated with linear loads, so the use of filters is more beneficial for nonlinear loads, where overshoot and unwanted oscillations are reduced. Active power with filtering has overshoot of 639.12 W, 278.45 W, and 1814.44 W for resistive, resistive-capacitive, and nonlinear loads, respectively, and a negative overshoot of 3.1 W for resistive-inductive loads. Therefore, unfiltered methods are more sensitive to load switching.

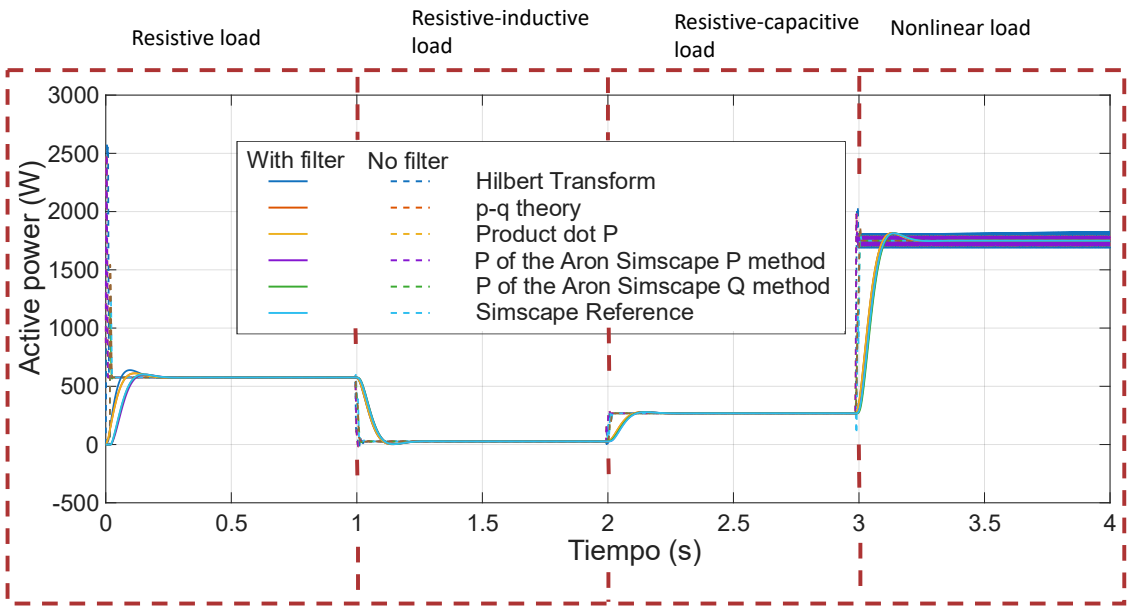


Figure 12. Active power with and without filtering.

doi: 10.25100/iyc.v28i3.16035

The filtered and unfiltered methods in Figure 13 show reactive power switching for 4 s. The unfiltered reactive power shows overshoots of 1214 VAR and 324.92 VAR for the resistive and resistive-capacitive loads, and exhibits negative overshoots of -258.7 VAR and -767.2 VAR for the resistive-inductive load and the nonlinear load.

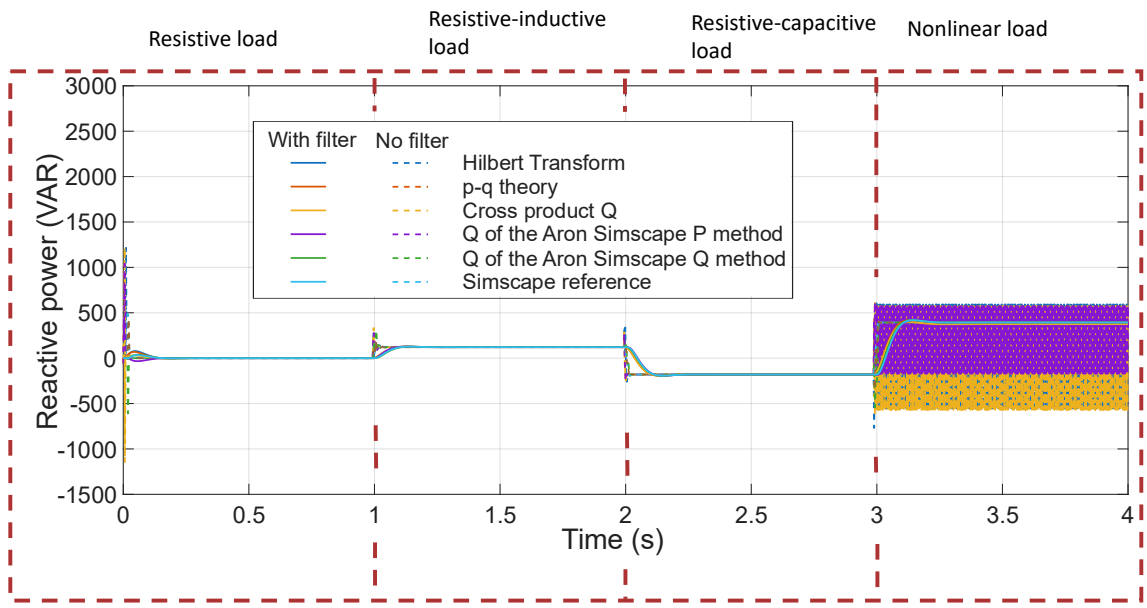


Figure 13. Reactive power with and without filtering.

The Hilbert transform exhibits the greatest overshoot and response delay, followed by the dot product method and *p-q* theory for the analyzed loads. At the end of the simulation for the nonlinear load, these methods maintain large oscillations. In contrast, Simscape's RMS methods have an initial overshoot with a stable termination for the nonlinear load. These methods, based on the Simscape reference, have an overshoot at a period of 0.0167 s for the resistive load. Reactive power with filtering has an overshoot of 77.69 VAR and 127.43 VAR for the resistive load, and a negative overshoot of -258.1 VAR for the resistive-inductive load. Maximum oscillations range between -767.2 and 623.3 VAR for the nonlinear load. The proposed filters prove effective in reducing overshoot and unwanted oscillations, especially for nonlinear loads.

Table 3 presents the performance of the seven methods for measuring active power without a filter. The indicators are the maximum error $\epsilon_{\max}$, MAE_s, RMSE_s, the relative error ϵ_r, the overshoot M_p and the settling time t_s without filtering. The seven methods are evaluated with resistive (R), resistive-inductive (RL), resistive-capacitive (RC), and nonlinear (NL) loads. For the R load, the methodologies based on *p-q* theory, the dot product, and the Hilbert transform register moderate relative errors between $0.587\ \%$ and $0.742\ \%$. However, they exhibit high overshoots of approximately $331.9\ \%$ and $350.3\ \%$ due to the absence of attenuation during the startup transient, with settling times of $0.0085\ \mathrm{s}$ to $0.0127\ \mathrm{s}$. For their part, the Aron-Simscape schemes manage to contain the MAE_s below $0.791\ \mathrm{W}$ and a RMSE_s of up to $10.1\ \mathrm{W}$.

doi: 10.25100/iyc.v28i3.16035

Table 3. Measurement methods with unfiltered active power indicators**.**

Method (Type of load)	ϵ_{max} (W)	MAE_s (W)	$RMSE_s$ (W)	ϵ_r (%)	M_p (%)	t_s (s)
p-q theory (R)	1911.5	3.382	36.1	0.587	331.9	0.0085
p-q theory (RL)	173.4	1.158	10.1	4.288	642.2	0.0587
p-q theory (RC)	1710.3	38.592	241.1	14.393	637.8	0.0085
p-q theory (NL)	40.9	23.846	26.7	1.363	2.1	0.8489
Dot product (R)	1911.5	3.382	36.1	0.587	331.9	0.0085
Dot product (RL)	173.4	1.158	10.1	4.288	642.2	0.0587
Dot product (RC)	1710.3	38.592	241.1	14.393	637.8	0.0085
Dot product (NL)	40.9	23.846	26.7	1.363	2.1	0.8489
Hilbert Transform (R)	1994.1	4.271	41.4	0.742	346.2	0.0127
Hilbert Transform (RL)	137.2	0.821	7.9	3.042	508.2	0.0613
Hilbert Transform (RC)	1774.7	34.945	233.8	13.032	661.9	0.0129
Hilbert Transform (NL)	85.1	48.174	53.1	2.753	4.9	0.8497
Two Wattmeter Method (R)	2017.7	4.960	46.5	0.861	350.3	0.0086
Two Wattmeter Method (RL)	174.0	0.883	8.7	3.271	644.3	0.0587
Two-wattmeter Method (RC)	2107.0	38.112	240.0	14.214	785.8	0.0084
Two Wattmeter Method (NL)	706.6	138.734	220.0	7.928	35.8	0.8499
P of the Aron Simscape *P* method (R)	575.7	0.791	8.8	0.137	96.3	0.0246
P of the Aron Simscape *P* method (RL)	400.1	0.207	0.6	0.768	1482.0	0.0536
P of the Aron Simscape *P* method (RC)	1135.7	14.546	105.8	5.425	423.5	0.0202
P of the Aron Simscape *P* method (NL)	345.3	0.112	0.1	0.006	3.0	0.0069
P of the Aron Simscape *Q* method (R)	703.6	0.752	10.1	0.131	122.1	0.0250
P of the Aron Simscape *Q* method (RL)	363.9	0.648	6.1	2.399	1347.7	0.0569
P of the Aron Simscape *Q* method (RC)	829.2	10.847	82.9	4.045	309.3	0.0185
P of the Aron Simscape *Q* method (NL)	710.3	0.116	0.1	0.007	5.1	0.0074
Simscape Reference (R)	967.5	1.227	13.9	0.213	168.0	0.0244
Simscape Reference (RL)	332.3	0.323	2.1	1.198	1230.6	0.0549
Simscape Reference (RC)	1219.6	15.536	114.1	5.794	454.8	0.0221
Simscape Reference (NL)	260.4	0.113	0.1	0.007	6.7	0.0081

Under RL load conditions, most methods exhibit a particular behavior in overshoots, which increase substantially, reaching values above $600\ \%$ in analytical models and exceeding $1200\ \%$ in the Aron-Simscape variants and the internal reference. However, under steady-state conditions, the values of MAE_s remain low between $0.207\ W$ and $1.158\ W$, with settling times around $0.053\ s$ to $0.061\ s$. RC load intensifies the error in all the analyzed methodologies. The classical and two-wattmeter

doi: 10.25100/iyc.v28i3.16035

algorithms reach RMSE_s high values, ranging between $233.8\ \mathrm{W}$ and $241.1\ \mathrm{W}$, with relative errors up to $14.393\ \%$ and overshoots greater than $600\ \%$. The Aron-Simscape variants reduce MAE_s to a range of $10.847\ \mathrm{W}$ to $15.536\ \mathrm{W}$ and a relative error bounded between $4.045\ \%$ and $5.794\ \%$. Furthermore, the impact of the lack of filtering creates a clear bifurcation for NL load. While the methods of *p-q* theory, dot product, Hilbert and two wattmeters suffer steady-state degradation with a value MAE_s that rises to $138.734\ \mathrm{W}$, the schemes based on Aron-Simscape and the Simscape reference neutralize this distortion by recording a MAE_s stable value of $0.112\ \mathrm{W}$ to $0.116\ \mathrm{W}$, a minimum relative error of $0.006\ \%$ to $0.007\ \%$ and very fast time responses of $0.0069\ \mathrm{s}$ to $0.0081\ \mathrm{s}$.

Table 4 presents the performance of the seven unfiltered reactive power measurement methods. The indicators present the $\epsilon_{\max}$, the MAE_s, RMSE_s and the $M_p$without filtering. For R loads, the methodologies based on *p-q* theory, the cross product, and the Hilbert transform register moderate relative errors between $1.69\ \%$ and $3.02\ \%$. These methodologies exhibit massive overshoots exceeding $100000\ \%$ due to the lack of attenuation in the initial transient and the use of initial values far from the solution. Settling times are short, ranging from $0.009\ \mathrm{s}$ to $0.013\ \mathrm{s}$. The schemes based on Aron-Simscape and the Simscape reference manage to keep the reactive power MAE_s below $1.45\ \mathrm{VAR}$ and a reactive power RMSE_s less than $15.16\ \mathrm{VAR}$. The behavior generally stabilizes for most algorithms for RL loads. For example, the Simscape reference has a MAE_s reactive power of $0.47\ \mathrm{VAR}$, a reactive power of RMSE_s $1.038\ \mathrm{VAR}$, and a relative error of $0.39\ \%$. However, the two-wattmeter method experiences degradation in steady state, reaching an MAE_s of $159.51\ \mathrm{VAR}$, an RMSE_s of $178.17\ \mathrm{VAR}$ and a settling time of $0.850\ \mathrm{s}$.

RC loading intensifies the dispersion among the analyzed techniques. Classical algorithms such as *p-q* theory and the cross product achieve values of RMSE_s and $90.85\ \mathrm{VAR}$, $94.85\ \mathrm{VAR}$ respectively. Meanwhile, the two-wattmeter method reports a MAE_s high $458.34\ \mathrm{VAR}$ and an overshoot of $2225\ \%$. In contrast, the Aron-Simscape variants and the internal reference maintain relative error control bounded between $1.97\ \%$ and $2.85\ \%$. Furthermore, the impact of the lack of filtering is evident in the data for NL loading. The cross product and the Hilbert transform achieve a MAE_s and $207.68\ \mathrm{VAR}$, $226.52\ \mathrm{VAR}$ with relative errors of up to $52.71\ \%$ and $57.49\ \%$, respectively. The settling time is $0.850\ \mathrm{s}$. The methods based on Aron-Simscape and the Simscape reference register a MAE_s of $0.29\ \mathrm{VAR}$, a ϵ_r of $0.07\ \%$ and fast time responses of $0.009\ \mathrm{s}$.

Table 5 presents active power indicators for the seven per-phase methods. The indicators are the $\epsilon_{\max}$, the MAE, the RMSE, the ϵ_r, the M_p and the t_s. The settling time is calculated with a tolerance of approximately 2%, and the subscript s is used to represent steady state. Methods based on *p-q* theory and the dot product yield identical results with $\mathrm{MAE}_s = 0.0021$ W and a $\mathrm{RMSE}_s = 0.0293$ W for the load R. The Hilbert transform and the two-wattmeter method have slightly higher errors. Implementations associated with Aron's method have a lower MAE of 10^{-3} W. Overshoot values M_p for this condition range from $4.4\ \%$ to $11\ \%$ depending on the method. The settling time for this condition is approximately between 0.169 s and 0.205 s. For the RL load, a homogeneous behavior is observed between the methodologies. The values of MAE_s remain around 0.1663 W and the RMSE_s presents values close to the MAE.

doi: 10.25100/iyc.v28i3.16035

Table 4. Measurement methods with unfiltered reactive power indicators

Method (Type of load)	ϵ_{max} (VAR)	MAE_s (VAR)	$RMSE_s$ (VAR)	ϵ_r (%)	M_p (%)	t_s (s)
p-q theory (R)	1040.6	2.55	23.359	2.55	104060.0	0.009
p-q theory (RL)	358.7	2.53	23.490	2.09	119.9	0.038
p-q theory (RC)	797.3	13.41	90.846	7.44	242.6	0.012
p-q theory (NL)	564.0	173.21	212.558	43.96	44.9	0.850
Cross product (R)	1215.2	3.02	28.029	3.02	121520.0	0.009
Cross product (RL)	358.9	2.63	24.027	2.18	135.6	0.038
Cross product (RC)	804.4	14.29	94.850	7.93	246.5	0.012
Cross product (NL)	963.8	207.68	329.268	52.71	45.0	0.850
Hilbert Transform (R)	1216.2	1.69	17.696	1.69	121620.0	0.013
Hilbert Transform (RL)	217.4	1.16	9.375	0.96	179.7	0.040
Hilbert Transform (RC)	786.1	12.77	88.079	7.09	326.8	0.016
Hilbert Transform (NL)	948.6	226.52	293.564	57.49	50.3	0.850
Two Wattmeter Method (R)	4556.7	727.67	811.345	727.67	455670.0	0.850
Two Wattmeter Method (RL)	625.3	159.51	178.170	131.83	516.8	0.850
Two-wattmeter Method (RC)	4369.0	458.34	602.979	254.40	2225.0	0.850
Two Wattmeter Method (NL)	3796.0	2237.30	2502.700	567.84	963.4	0.850
Q of the Aron Simscape *P* method (R)	609.4	1.45	15.151	1.45	60937.0	0.025
Q of the Aron Simscape P method (RL)	186.5	0.63	2.700	0.52	154.1	0.042
Q of the Aron Simscape *P* method (RC)	362.8	4.41	32.743	2.45	201.4	0.022
Q of the Aron Simscape *P* method (NL)	651.8	0.29	0.289	0.07	0.0	0.009
Q of the Aron Simscape *Q* method (R)	488.1	0.31	3.116	0.31	48809.0	0.025
Q of the Aron Simscape *Q* method (RL)	72.1	0.56	2.226	0.46	11.3	0.033
Q of the Aron Simscape *Q* method (RC)	409.2	5.13	38.549	2.85	27.1	0.018
Q of the Aron Simscape *Q* method (NL)	164.6	0.29	0.289	0.07	8.2	0.009
Simscape Reference (R)	431.4	0.69	6.796	0.69	43138.0	0.025
Simscape Reference (RL)	82.1	0.47	1.038	0.39	51.5	0.034
Simscape Reference (RC)	303.0	3.56	25.452	1.97	90.7	0.024
Simscape Reference (NL)	424.3	0.29	0.288	0.07	3.6	0.009

The relative error is approximately between 0.615 and 0.617%. Likewise, a noticeable increase in overshoot is recorded for this load due to the inductive dynamics, reaching values higher than. Settling times increase compared to the resistive load and are approximately between 0.3125 s and 0.321 s. The RC load shows pronounced differences between the methodologies, reaching values higher than 2020%. *p-q* theory, the dot product and the two-wattmeter method present the $RMSE_s$

doi: 10.25100/iyc.v28i3.16035

between approximately 6.38 W and 6.49 W. The Hilbert transform reduces it to 4.69 W, and RMSE_s Aron MAE_s's methods show a reduction of the method associated with **Q**. The MAE is 0.0452 W and its RMSE is 0.4993 W. The relative error is 0.0167 %. Settling times remain within a relatively narrow range, approximately between 0.1835 s and 0.1938 s. The values of $E_{\max}$ are on the order of 10^3 W for the NL load. Steady-state errors are smaller. Most methodologies present values of MAE_s close to 0.11 W with relative errors on the order of 0.006% to 0.007%. The two-wattmeter method shows an increase in error that reaches a $\mathrm{MAE}_s = 0.2225$ W and a $\mathrm{RMSE}_s = 0.2533$ W. The overshoot for nonlinear loads remains stable and low, consistently hovering around $3.6\ \%$ to $3.7\ \%$. Settling times for this condition are approximately between 0.1733 s and 0.1842 s. The greatest differences between methodologies are observed in the RC load and the R, RL, and NL loads. These R, RL, and NL estimates are closer to each other. The settling times show a significant dependence on the load type, with the RL condition exhibiting the highest values in virtually all the evaluated methodologies.

doi: 10.25100/iyc.v28i3.16035

Table 5. Measurement methods with active power indicators with filter

Method (Type of load)	$\epsilon_{\max}$ (W)	MAE_s (W)	RMSE_s (W)	ϵ_r (%)	M_p (%)	t_s (s)
p-q theory (R)	576.0	0.002	0.0293	0.0004	6.1	0.1742
p-q theory (RL)	548.1	0.166	0.1668	0.6162	2029.9	0.314
p-q theory (RC)	240.6	0.762	6.4937	0.2842	33.7	0.1835
p-q theory (NL)	1391.4	0.113	0.1128	0.0064	3.7	0.1737
Dot product (R)	576.0	0.002	0.0293	0.0004	6.1	0.1742
Dot product (RL)	548.1	0.166	0.1668	0.6162	2029.9	0.314
Dot product (RC)	240.6	0.762	6.4937	0.2842	33.7	0.1835
Dot product (NL)	1391.4	0.113	0.1128	0.0064	3.7	0.1737
Hilbert Transform (R)	576.0	0.006	0.0714	0.0010	11.0	0.1693
Hilbert Transform (RL)	547.0	0.166	0.1662	0.6153	2026.0	0.3135
Hilbert Transform (RC)	241.1	0.507	4.6901	0.1890	26.6	0.1875
Hilbert Transform (NL)	1410.4	0.112	0.1138	0.0064	3.7	0.1749
Two Wattmeter Method (R)	576.0	0.007	0.1009	0.0012	5.8	0.1753
Two Wattmeter Method (RL)	546.3	0.167	0.1666	0.6168	2023.5	0.3125
Two-wattmeter Method (RC)	241.3	0.746	6.3845	0.2783	33.4	0.1841
Two Wattmeter Method (NL)	1392.3	0.223	0.2533	0.0127	3.7	0.1733
P of the Aron Simscape *P* method (R)	576.0	0.001	0.0068	0.0002	4.4	0.2047
P of the Aron Simscape *P* method (RL)	548.8	0.166	0.1664	0.6165	2032.6	0.3208
P of the Aron Simscape *P* method (RC)	241.3	0.136	1.3176	0.0509	8.3	0.1925
P of the Aron Simscape *P* method (NL)	1459.6	0.112	0.1123	0.0064	3.6	0.1823
P of the Aron Simscape *Q* method (R)	576.0	0.001	0.005	0.0002	4.6	0.2009
P of the Aron Simscape *Q* method (RL)	549.1	0.166	0.1662	0.6153	2033.7	0.321
P of the Aron Simscape *Q* method (RC)	241.2	0.045	0.4993	0.0167	3.9	0.1906
P of the Aron Simscape *Q* method (NL)	1471.4	0.116	0.116	0.0066	3.6	0.1842
Simscape Reference (R)	576.0	0.001	0.0085	0.0002	4.6	0.1999
Simscape Reference (RL)	548.7	0.166	0.1664	0.6163	2032.3	0.3197
Simscape Reference (RC)	241.3	0.138	1.3979	0.0516	8.9	0.1938
Simscape Reference (NL)	1457.9	0.113	0.1129	0.0064	3.7	0.1813

Table 6 presents performance indicators for the seven reactive power measurement methods. The maximum error $\epsilon_{\max}$, the MAE_s, the RMSE_s, the relative error ϵ_r, the M_p and the t_s are calculated for different types of loads per phase. The settling time is calculated with a tolerance of 2%. The four load conditions are R, RL, RC, and NL loads. For load R, the smallest steady-state errors are observed for most methodologies. The ***p-q*** theory presents a MAE_s of 0.0049 VAR and an RMSE_s

doi: 10.25100/iyc.v28i3.16035

of 0.0696 VAR. The Aron-Simscape methods have minor errors; the method associated with Q achieves a MAE_s of 4.65×10^{-4} VAR and a RMSE_s of 0.0045 VAR. The overshoot for this resistive condition has high values due to the initial startup transient, ranging between $3061.6\ \%$ and $12881\ \%$ according to the method. The settling time for this condition is between 0.1303 and 0.2391 s.

Table 6. Measurement methods with reactive power indicators with filter

Method (Type of load)	$\epsilon_{\max}$ (VAR)	MAE_s (VAR)	RMSE_s (VAR)	ϵ_r (%)	M_p (%)	t_s (s)
p-q theory (R)	68.9	0.005	0.070	0.0049	6886.9	0.2165
p-q theory (RL)	119.2	0.393	0.393	0.3244	4.9	0.1856
p-q theory (RC)	301.2	0.229	2.017	0.1269	7.3	0.2012
p-q theory (NL)	544.8	0.288	0.290	0.0732	6.2	0.1917
Cross product (R)	30.6	0.006	0.089	0.0061	3061.6	0.1303
Cross product (RL)	118.8	0.393	0.393	0.3246	5.0	0.1835
Cross product (RC)	301.3	0.211	1.866	0.1172	7.3	0.2012
Cross product (NL)	546.7	19.471	19.472	4.9419	1.2	0.85
Hilbert Transform (R)	77.8	0.006	0.079	0.0058	7775.1	0.2261
Hilbert Transform (RL)	119.2	0.394	0.394	0.3254	4.8	0.1881
Hilbert Transform (RC)	302.0	0.052	0.398	0.0287	7.3	0.2047
Hilbert Transform (NL)	569.7	0.265	0.281	0.0671	6.3	0.1971
Two Wattmeter Method (R)	128.8	0.013	0.195	0.0134	12881.0	0.2391
Two Wattmeter Method (RL)	116.1	0.394	0.394	0.3254	5.6	0.1766
Two-wattmeter Method (RC)	301.2	0.136	1.074	0.0756	7.3	0.2049
Two Wattmeter Method (NL)	578.4	0.288	0.291	0.0731	6.3	0.1997
Q of the Aron Simscape *P* method (R)	33.0	0.001	0.015	0.0011	3301.8	0.147
Q of the Aron Simscape *P* method (RL)	120.5	0.393	0.393	0.3244	5.6	0.1848
Q of the Aron Simscape *P* method (RC)	301.6	0.030	0.273	0.0164	7.2	0.213
Q of the Aron Simscape *P* method (NL)	577.6	0.289	0.289	0.0733	6.2	0.2081
Q of the Aron Simscape *Q* method (R)	37.5	0.000	0.005	0.0005	3749.5	0.1493
Q of the Aron Simscape *Q* method (RL)	120.9	0.393	0.393	0.3244	4.7	0.1981
Q of the Aron Simscape *Q* method (RC)	301.6	0.042	0.419	0.0232	7.2	0.2098
Q of the Aron Simscape *Q* method (NL)	566.8	0.290	0.290	0.0735	6.2	0.1997
Simscape Reference (R)	33.1	0.001	0.012	0.0009	3309.7	0.1487
Simscape Reference (RL)	120.7	0.393	0.393	0.3245	4.7	0.1945
Simscape Reference (RC)	301.7	0.021	0.171	0.0118	7.2	0.2111
Simscape Reference (NL)	574.6	0.288	0.288	0.0730	6.2	0.2039

doi: 10.25100/iyc.v28i3.16035

For RL, the differences between the methodologies are considerably smaller. MAE_s remains between 0.3925 VAR and 0.394 VAR and the RMSE_s presents practically equivalent values. The relative error is around between 0.324% and 0.325%. The overshoot is significantly reduced in this inductive condition, oscillating stably between 4.7 % and 5.6 %. Settling times range between 0.1766 s and 0.1981 s, demonstrating a relatively similar time response among the evaluated methods. The RC load shows the most significant differences between the methodologies. *p-q* theory presents a RMSE_s of 2.0165 VAR and the cross product reaches 1.8655 VAR. The two-wattmeter method reduces this indicator to 1.0739 VAR. These results show that the RC load condition generates greater error dispersion among the methodologies. Most methods present values MAE_s close to 0.021 VAR and 0.229VAR and relative errors close to $0.0118\ \%$. $0.1269\ \%$, Likewise, the overshoot in the capacitive condition remains consistently bounded around $7.2\ \%$ to $7.3\ \%$ for all variants. However, the cross-product Q constitutes a notable exception, with a $\mathrm{MAE}_s = 19.4710\ \mathrm{VAR}$, a $\mathrm{RMSE}_s = 19.4715\ \mathrm{VAR}$, a relative error of $4.9419\ \%$, an overshoot of $1.2\ \%$ and a settling time of $0.85\ \mathrm{s}$. The remaining methodologies maintain settling times below approximately 0.21 s and relative errors close to the value obtained using the Simscape reference. Furthermore, for the nonlinear (NL) load condition, the overshoot stabilizes in a moderate range $1.2\ \%$ to $6.3\ \%$.

On the one hand, active power methodologies exhibit high overshoots and errors during switching and transient disturbances without filtering. In contrast, low-pass filters attenuate these effects and stabilize the active power MAE_s below 0.22 W in steady state, allowing for a more accurate estimation of the average active power. On the other hand, the absence of filtering generates overshoots and oscillations in reactive power during transients and abrupt load changes. The incorporation of filters reduces these fluctuations and maintains the MAE_s below 0.29 VAR. Although unfiltered methods preserve instantaneous dynamics, filtering favors a more stable response.

Conclusions

This research aims to review the temporal behavior, application, and formulation of seven methodologies, developing seven methods for measuring instantaneous complex power in balanced three-phase systems on a single test platform. The conclusions confirming the known methodologies are presented below. Instantaneous complex powers are calculated using *p-q* theory, the two-wattmeter method, and cross-vector theory, which numerically coincide with the average values of active and reactive power. The methodology integrates theories based on the Clarke *p-q* transform and the dot product *p*, along with cross-vector theory *q*, which exhibit virtually identical error curves for linear resistive, resistive-capacitive, and resistive-inductive loads. Furthermore, the adaptation of the two-wattmeter method, also known as the Aron method, is used to estimate instantaneous power and represents a practical advancement, especially for systems without a neutral conductor. Analytical formulations allow us to examine the nature of these methods, in which the fundamental frequency component is canceled, thus enabling the estimation of instantaneous complex power. The implications of this study suggest that the cross-

doi: 10.25100/iyc.v28i3.16035

vector method provides a conceptual framework for the analysis of complex systems in electrical networks.

The conclusions that present new contributions derived from this research are stated below. Aron's method exhibits greater numerical sensitivity and continuous oscillations when reactive power is close to zero, indicating that its use requires more careful filtering, such as the use of band-stop filters. The analysis includes the accuracy and numerical stability of the methods, proposing the use of a logarithmic scale, which provides greater sensitivity for analyzing diverse load conditions. These conditions include resistive, resistive-capacitive, resistive-inductive, and nonlinear loads. Furthermore, the study addresses the use of filters for balanced three-phase positive-sequence systems, presenting their formulation, constants, and computational simulation, demonstrating their value for the study. This study considers that instantaneous complex powers produce time delays consisting of an overshoot and power settling time. In fact, a band-stop filter is used to reduce the second harmonic in the two-wattmeter method. Regarding performance with nonlinear loads, the study concludes that these pose the greatest challenge to measurement accuracy. It is worth noting that, with the use of filters, all seven methods maintain an absolute error for active power below 0.6 W and an absolute error for reactive power below 0.3 VAR in steady state. Furthermore, the Hilbert transform appears to have a slightly higher accuracy limit compared to instantaneous theories. Additionally, the integration of second-order low-pass filters with a Butterworth response is crucial in all methodologies to stabilize the signals and effectively distinguish between average and oscillatory components. Under steady-state conditions for both linear and non-linear loads, the methodologies succeed in keeping the mean absolute error MAE_s below 0.22 W for active power and below 0.29 VAR for reactive power. The mean square error RMSE_s is below 0.25 W for active power and 0.29 VAR for reactive power, except for the cross-vector theory in Q which reaches 19.47 VAR due to harmonic distortion and the relative percentage errors are below 0.62% for active power and 0.33% for reactive power under linear load conditions.

Future research could delve deeper into the comparison of unbalanced three-phase systems with harmonic distortion at the source, where the limitations of traditional *p-q* theory become more apparent. Furthermore, the computational efficiency of these methods can be studied to improve the operation of electrical grids. Monitoring power quality issues can be integrated with these methodologies, enhancing the management of electrical grids with reactive power compensation.

CRediT authorship contribution statement

Conceptualization - Ideas: Edison Andrés Caicedo Peñaranda, Pedro Julian Garcia-Guarin. Data curation: Edison Andrés Caicedo Peñaranda, Pedro Julian Garcia-Guarin. Formal Analysis: DEdison Andrés Caicedo Peñaranda, Pedro Julian Garcia-Guarin. Investigation: Edison Andrés Caicedo Peñaranda, Pedro Julian Garcia-Guarin. Methodology: Edison Andrés Caicedo Peñaranda, Pedro Julian Garcia-Guarin. Project Management: Edison Andrés Caicedo Peñaranda, Pedro Julian Garcia-Guarin. Resources: Edison Andrés Caicedo Peñaranda, Pedro Julian Garcia-Guarin. Supervision: Diego León Peña Orozco. Validation: Edison Andrés Caicedo Peñaranda, Pedro Julian Garcia-Guarin. Writing - original draft - Preparation: Edison Andrés Caicedo Peñaranda, Pedro Julian Garcia-Guarin. Writing - revision and editing - Preparation: Edison Andrés Caicedo Peñaranda, Pedro Julian Garcia-Guarin.

doi: 10.25100/iyc.v28i3.16035

Financing: The authors declare that no external funding was received. Conflict of interest: The authors declare no conflicts of interest. Ethical aspect: Not applicable.

References

1. Salmerón P, Herrera RS. Instantaneous reactive power theory-A general approach to poly-phase systems [Internet]. Vol. 79, Electric Power Systems Research. 2009 [cited 2026 Feb 13]. p. 1263-70.

https://doi.org/10.1016/j.epsr.2009.03.007

2. Tahri A, Draou A. Instantaneous Active and Reactive Power Measuring Method in Three Phase Power System. Leonardo Electron J Pract Technol [Internet]. 2005 [cited 2026 Feb 13];(6):17-28.

https://lejpt.academicdirect.org/A06/17_28.htm

3. Mikkili S, Panda AK. Instantaneous Active and Reactive Power and Current Strategies for Current harmonics cancellation in 3-ph 4wire SHAF With both PI and Fuzzy Controllers. Energy Power Eng [Internet]. 2011 [cited 2026 Feb 13];03(03):285-98.

https://doi.org/10.4236/epe.2011.33036

4. Akagi H, Kanazawa Y, Nabae A. Instantaneous Reactive Power Compensators Comprising Switching Devices without Energy Storage Components. IEEE Trans Ind Appl [Internet]. 1984 [cited 2026 Feb 13];IA-20(3):625-30. Available from:

https://doi.org/10.1109/TIA.1984.4504460

5. Satish G, Rameshkumar K, Dhanasakkaravarthi B, Jeyalakshmi K, Chaudhary S, Singh N. Non-Linear Controller Based 3- □ Shunt Active Filter for Improvement of Power Quality in Non-Linear Load. In: 2023 IEEE International Conference on Integrated Circuits and Communication Systems, ICICACS 2023 [Internet]. Institute of Electrical and Electronics Engineers Inc.

https://doi.org/10.1109/ICICACS57338.2023.10099957

6. Caicedo Peñaranda, E.A, Muegues Serrano H., García Guarin J. Estimador de potencia instantánea en sistemas eléctricos monofásicos. In: XVII Congreso Internacional de Electrónica y Tecnologías de Avanzada. 2025. p. 7.

7. Herrera RS, Salmeron P. Instantaneous reactive power theory: A comparative evaluation of different formulations. IEEE Trans Power Deliv [Internet]. 2007 Jan [cited 2026 Feb 17];22(1):595-604. Available from:

https://doi.org/10.1109/TPWRD.2006.881468

8. Ustariz-Farfan AJ, Cano-Plata EA, Tacca HE. Teoría generalizada de la potencia instantánea aplicada a la compensación de cargas polifásicas. Ingeniare Rev Chil Ing [Internet]. 2012 [cited 2026 Feb 19];20(2):148-59.

https://doi.org/10.4067/S0718-33052012000200002

9. Yu Y, Zhao W, Li S, Huang S. A Two-Stage Wavelet Decomposition Method for Instantaneous Power Quality Indices Estimation Considering Interharmonics and Transient Disturbances. IEEE Trans Instrum Meas [Internet]. 2021 [cited 2026 Feb 13];70.

https://doi.org/10.1109/TIM.2021.3052554

10. Kirkham H, Strickland D, Berrisford A, Bihler M, Britton J, Kirby R, et al. IEEE 1459 - Standard Definitions for the Measurement of Electric Power Quantities Under Sinusoidal, Nonsinusoidal, Balanced, or Unbalanced Conditions. IEEE Std 1459-2025 (Revision IEEE Std 1459-2010) [Internet]. 2025 [cited 2026 Jun 10];1-61.

doi: 10.25100/iyc.v28i3.16035

https://ieeexplore.ieee.org/document/11004570/

11. Peng FZ, Huang H, Tolbert LM, Lehman B, Li YA. Spacetime pq theory for AC and DC electric power systems. Sci Rep [Internet]. 2025 [cited 2026 Feb 17];15(1). Available from:

https://doi.org/10.1038/s41598-025-90021-3

12. Artemenko MY, Kutafin Y V., Mykhalskyi VM, Chopyk V V., Shapoval IA, Polishchuk SY. Control Strategies for Three-Phase Three-Wire Shunt Active Filter in the Reference Frame of Two-Wattmeter Method. In: Proceedings - IEEE International Conference on Electronics and Nanotechnology, ELNANO [Internet]. 2020 [cited 2026 Feb 13]. p. 780-5.

https://doi.org/10.1109/ELNANO50318.2020.9088885

13. Memon ZA, Uqaili MA, Unar A. Design of Three-Phase Hybrid Active Power Filter for Compensating the Harmonic Currents of Three-Phase System [Internet]. Vol. 31, Mehran University Research Journal of Engineering & Technology. 2012 Apr [cited 2026 Feb 13].

https://arxiv.org/pdf/1604.03223

14. Rajashekaraiah K, De Carne G, Iurlaro C, Semeraro M, Bruno S. P-Q Theory-based Dynamic Load Modelling in Short-Circuit Analysis. In: 2023 8th IEEE Workshop on the Electronic Grid, eGRID 2023 [Internet]. 2023 [cited 2026 Feb 17].

https://doi.org/10.1109/eGrid58358.2023.10380853

15. Artemenko M, Chopyk V, Polishchuk S, Mykhalskyi V, Shapoval I. Integral Power Theory and Active Filtering Using the □-□ Reference Frame. IEEE Access [Internet]. 2024 [cited 2026 Feb 13];12:60004-14. Available from:

https://doi.org/10.1109/ACCESS.2024.3393767

16. Montoya FG, Alcayde A, Arrabal-Campos FM, Banos R. How to overcome the limitations of p-q Theory: Geometric algebra power theory to the rescue. In: IEEE PES Innovative Smart Grid Technologies Conference Europe [Internet]. 2020 [cited 2026 Feb 14]. p. 339-43.

https://doi.org/10.1109/ISGT-Europe47291.2020.9248978

17. Czarnecki LS. Instantaneous reactive power p-q theory and power properties of three-phase systems. IEEE Trans Power Deliv [Internet]. 2006 Jan [cited 2026 Feb 13];21(1):362-7.

https://doi.org/10.1109/TPWRD.2005.852348

18. Akagi H, Ogasawara S, Kim H. The theory of instantaneous power in three-phase four-wire systems and its applications. Electr Eng Japan (English Transl Denki Gakkai Ronbunshi) [Internet]. 2001 May [cited 2026 Feb 17];135(3):74-86. Available from:

https://doi.org/10.1002/eej.1035

19. Herrera RS, Salmerón P, Vázquez JR, Litrán SP, Pérez A. Generalized instantaneous reactive power theory in poly-phase power systems. In: 2009 13th European Conference on Power Electronics and Applications, EPE '09 [Internet]. 2009 [cited 2026 Feb 17].

https://ieeexplore.ieee.org/abstract/document/5279292/

20. Fiorucci E. The measurement of actual apparent power and actual reactive power from the instantaneous power signals in single-phase and three-phase systems. Electr Power Syst Res [Internet]. 2015 Apr 1 [cited 2026 Feb 17];121:227-42. Available from:

https://doi.org/10.1016/j.epsr.2014.11.002

doi: 10.25100/iyc.v28i3.16035

21. Kumar SS, Arya K, Chandrakala KRMV, Nadar KP. Implementation of Instantaneous P-Q Theory to Improve Power Quality by Shunt Active Power Filter for Non-Linear Loads. In: 2024 IEEE 3rd International Conference on Electrical Power and Energy Systems, ICEPES 2024 [Internet]. 2024 [cited 2026 Feb 13]. Available from:

https://doi.org/10.1109/ICEPES60647.2024.10653568

22. Akagi H, Watanabe EH, Aredes M. The Instantaneous Power Theory. In: Instantaneous Power Theory and Applications to Power Conditioning [Internet]. John Wiley & Sons, Ltd; 2017 [cited 2026 Feb 17]. p. 37-109. Available from:

https://doi.org/10.1002/9781119307181.ch3

23. Mikulovi J, Šekara T, Forcan M. Power definitions for three-phase systems in terms of instantaneous symmetrical components. Int J Electr Power Energy Syst [Internet]. 2023 [cited 2026 Feb 17];147. Available from:

https://doi.org/10.1016/j.ijepes.2022.108808

24. Aguilera RP, Acuña P, Rojas C, Pou J, Konstantinou G, Watanabe EH. An Instantaneous Power Theory Extension for the Interphase Power Imbalance Problem. IEEE Trans Power Electron [Internet]. 2024 [cited 2026 Feb 17];39(10):12261-70.

https://doi.org/10.1109/TPEL.2024.3397788

25. Salmerón P, Herrera RS, Vázquez JR. A new approach for three-phase loads compensation based on the instantaneous reactive power theory. Electr Power Syst Res [Internet]. 2008 [cited 2026 Feb 17];78(4):605-17. Available from:

https://doi.org/10.1016/j.epsr.2007.05.003

26. Lu Z, Yan W, Huang D, Tang J, Ponci F, Monti A. State Estimation for Medium- and Low-Voltage Distribution Systems Considering Measurement Characteristics and Grounded Slack Bus. IEEE Trans Instrum Meas [Internet]. 2022 [cited 2026 Feb 13];71.

https://doi.org/10.1109/TIM.2022.3214285

27. Czarnecki LS. Constraints of instantaneous reactive power p-q theory. IET Power Electron [Internet]. 2014 Sep 1 [cited 2026 Feb 13];7(9):2201-8. Available from:

https://doi.org/10.1049/iet-pel.2013.0579

28. Czarnecki LS. On some misinterpretations of the instantaneous reactive power p-q theory. IEEE Trans Power Electron [Internet]. 2004 [cited 2026 Feb 13];19(3):828-36.

https://doi.org/10.1109/TPEL.2004.826500

29. Aredes M, Akagi H, Watanabe EH, Salgado EV, Encarnação LF. Comparisons between the p-q and p-q-r theories in three-phase four-wire systems. IEEE Trans Power Electron [Internet]. 2009 [cited 2026 Feb 17];24(4):924-33.

https://doi.org/10.1109/TPEL.2008.2008187

30. Vinifa R, Kavitha A, Selwynraj A. A Comparison of Instantaneous and Extension p-q Methods for Current Controlled Voltage Source Inverter in Microgrid. Int J Electron [Internet]. 2022 [cited 2026 Feb 18];109(11):1896-914. Available from:

https://doi.org/10.1080/00207217.2021.2001859

31. Urrego A, Laiseca S. Estudio experimental de potencias, factor de potencia y energía eléctrica en cargas industriales tomando como referencia la norma IEEE Std 1459-2010. Tecnura [Internet]. 2015

doi: 10.25100/iyc.v28i3.16035

[cited 2026 Feb 17];19(1):1-14.

http://www.scielo.org.co/scielo.php?pid=S0123921X2015000500004&script=sci_arttext

32. Van Tung L, Huy DN, Huyen LT. Comparison of Power Grid Quality Using Active Filter Control Based on P-Q Power Theory and D-Q Rotating Reference Frame Under Nonlinear Load Conditions. Proc - 2025 Int Ural Conf Electr Power Eng Ural 2025 [Internet]. 2025 [cited 2026 Feb 17];759-66.

https://doi.org/10.1109/UralCon67204.2025.11206610

33. Jauhari M, Ilman AF, Prasetyani L, Dewi T. Control Strategy for Active Power Filter Based on P-Q Theory under Non-Ideal Mains Voltages. In: Proceeding - 2020 2nd International Conference on Industrial Electrical and Electronics, ICIEE 2020 [Internet]. 2020 [cited 2026 Feb 17]. p. 31-5.

https://doi.org/10.1109/ICIEE49813.2020.9276891

34. Zou X, Sheng Y, Jiang Y. Research on active power filter technology. In: Journal of Physics: Conference Series [Internet]. IOP Publishing; 2023 [cited 2026 Feb 19]. p. 12002. h

ttps://iopscience.iop.org/article/10.1088/1742-6596/2477/1/012002/meta

35. Parton JE. The measurement of power factor, and active and reactive power, of balanced n -phase n -wire systems. Proc IEE - Part IV Inst Monogr [Internet]. 1952 Dec [cited 2026 Feb 17];99(4):358-66.

https://doi.org/10.1049/pi-4.1952.0036

36. Ding W, Zhang D, Huang W, Zhong C. The two-wattmeter method of measuring electrical power based on TMS320F2812. In: 2011 International Conference on Computer Science and Service System, CSSS 2011 - Proceedings [Internet]. 2011 [cited 2026 Feb 19]. p. 910-3.

https://doi.org/10.1109/CSSS.2011.5973943

37. Beck Y, Calamaro N, Shmilovitz D. A review study of instantaneous electric energy transport theories and their novel implementations [Internet]. Vol. 57, Renewable and Sustainable Energy Reviews. 2016 [cited 2026 Feb 17]. p. 1428-39. Available from:

https://doi.org/10.1016/j.rser.2015.12.086